HHS Public Access

Author manuscript

Nat Commun. Author manuscript; available in PMC 2014 December 16.

Published in final edited form as:

Nat Commun. ; 5: 5383. doi:10.1038/ncomms6383.

The Estrogen receptor alpha-regulated lncRNA NEAT1 is a critical modulator of prostate cancer

Dimple Chakravarty[1,3], **Andrea Sboner**[1,2,3], **Sujit S Nair**[4], **Eugenia Giannopoulou**[5,6], **Ruohan Li**[7], **Sven Hennig**[8], **Juan Miguel Mosquera**[1,3], **Jonathan Pauwels**[1], **Kyung Park**[1], **Myriam Kossai**[1,3], **Theresa Y. MacDonald**[1], **Jacqueline Fontugne**[1,3], **Nicholas Erho**[9], **Ismael A. Vergara**[9], **Mercedeh Ghadessi**[9], **Elai Davicioni**[9], **Robert B. Jenkins**[10], **Nallasivam Palanisamy**[11], **Zhengming Chen**[12], **Shinichi Nakagawa**[13], **Tetsuro Hirose**[14], **Neil H. Bander**[15], **Himisha Beltran**[1,3], **Archa H. Fox**[7], **Olivier Elemento**[2,3], and **Mark A Rubin**[1,3,*]

[1]Department of Pathology and Laboratory Medicine, Weill Medical College of Cornell University

[2] Institute for Computational Medicine, Weill Cornell Medical College of Cornell University

[3] Institute for Precision Medicine, Weill Medical College of Cornell University & New York Presbyterian Hospital

[4]Department of Biochemistry and Molecular Biology, School of Medicine and Health Sciences, George Washington University, Washington DC, USA

[5] Biological Sciences Department, New York City College of Technology, City University of New York

[6]Arthritis and Tissue Degeneration Program and the David Z. Rosensweig Genomics Research Center, Hospital for Special Surgery

[7]School of Biomedical, Biomolecular, and Chemical Sciences, University of Western Australia, Crawley, Western Australia 6009, Australia

[8]Chemical Genomics Centre, Dortmund, Germany

[9]Research and Development, GenomeDx Biosciences, Vancouver, British Columbia, Canada

[10]Department of Pathology and Laboratory Medicine, Mayo Clinic, Rochester, Minnesota

[11]Michigan Center for Translational Pathology, University of Michigan, Ann Arbor, MI 48105

[12]Division of Biostatistics and Epidemiology, Department of Public Health, Weill Cornell Medical College

*Correspondence: rubinma@med.cornell.edu.

Author contributions: Conception and design: D.C., S.S.N and M.A.R. Development of reagents and methodology: D.C., S.S., A.S., A.H.F., S.N, T.H., R.L., S.H., N.P., N.H.B. Acquisition of data: D.C., A.S., K. P., Z.C., N.E., I.A.V., M.G., E.D., R.B.J., T.Y.M, J.F., J.P., M.K. Analysis and interpretation of data: D.C., A.S., S.S.N., J.M.M., E.G., M.A.R. Writing, review and/or revision of the manuscript: D.C., S.S.N., A.S., O.E., H.B., M.A.R. Administrative, technical, or material support (i.e., reporting or organizing data, constructing databases): D.C., A.S., M.A.R. Study supervision: M.A.R.

Competing financials interests: The authors declare no competing financial interests.

Accession codes: Genome-wide data generated in this study have been deposited with The Gene Expression Omnibus (GEO) under accession no. GSE43988

[13]RNA Biology Laboratory, RIKEN Advanced Research Institute, Wako, Saitama, Japan Banting

[14]Functional RNomics Team, Biomedicinal Information Research Center, National Institute of Advanced Industrial Science and Technology (AIST), 2-4-7 Aomi, Koutou, Tokyo, Japan

[15] Department of Urology, Weill Cornell Medical College of Cornell University.

Abstract

The androgen receptor (AR) plays a central role in establishing an oncogenic cascade that drives prostate cancer progression. Some prostate cancers escape androgen dependence and are often associated with aggressive phenotype. The estrogen receptor alpha (ERα) is expressed in prostate cancers, independent of AR status. However, the role of ERα remains elusive. Using a combination of chromatin immunoprecipitation (ChIP) and RNA-sequencing data, we identified an ERα specific non coding transcriptome signature. Amongst putatively ERα-regulated intergenic long non coding RNAs (lncRNAs), we identified Nuclear Enriched Abundant Transcript 1 (NEAT1) as the most significantly overexpressed lncRNA in prostate cancer. Analysis of two large clinical cohorts also revealed that NEAT1 expression is associated with prostate cancer progression. Prostate cancer cells expressing high levels of NEAT1 were recalcitrant to androgen or AR antagonists. Finally, we provide evidence that NEAT1 drives oncogenic growth by altering the epigenetic landscape of target gene promoters to favor transcription.

Steroid receptors are key transducers of hormone signaling and control a wide spectrum of tissue-specific functions that are critical for physiological homeostasis of reproductive organs. Aberrant or deregulated expressions of steroid nuclear receptors are often associated with cancer progression and have been a major target for therapeutic intervention. The androgen receptor (AR) plays a central role in the progression of prostate cancer[1]. Androgen ablation is highly effective in treating metastatic prostate cancer, though resistance inevitably develops leading to castrate-resistant prostate cancer (CRPC). Most cases of CRPC remain dependent on AR signaling, which has led to the clinical development and recent approval of potent AR-targeted therapies for CRPC (i.e., abiraterone, enzalutamide)[2,3]. However, similar to first-generation anti-androgen therapies, patients develop resistance to these second-generation hormonal therapies. How CRPC tumors bypass AR signaling is emerging as a significant area of investigation. Many view co-targeting therapies as an important next step to managing the inevitable emergence of resistance to single-agent treatments, but critical to co-targeting is the identification of other biological pathways that drive disease progression and the development of strategies that can target judgmental pathways.

In CRPC, crosstalk between estrogen- and androgen-signaling pathways may present an opportunity for clinical intervention. Estrogen receptor (ER) signaling through ER alpha ($ER\alpha$) increases with prostate cancer progression[4-6] and can drive important oncogenic events, including TMPRSS2-ERG expression[7]. Although ERα signaling has been extensively studied in breast cancer[8-10], our understanding of the potential impact of this nuclear receptor on prostate physiology is less clear. Nevertheless, the connection is a particularly intriguing concept given that most cases of prostate cancer arise in the sixth

decade of life, a time when testosterone levels are decreasing and estrogens are increasing in men. Mouse models suggest that antagonism of ERα may diminish prostate carcinogenesis[4].

We posit that ERα is an important alternate signaling pathway for the transcriptional regulation of prostate cancer, allowing refractory disease to bypass androgen/AR signaling. Herein, we provide experimental evidence to support this hypothesis and demonstrate a functional specialization and distinct genomic role of this nuclear receptor in prostate cancer, with significant implications for prognosis and management. We show that ERα is recruited to both coding and non-coding regions of the prostate genome and orchestrates expression of non-coding regulatory RNAs.

We identified Nuclear Enriched Abundant Transcript 1 (NEAT1) long non-coding RNA (lncRNA) as a potential target of ERα and as an important mediator for maintenance of prostate cancer. NEAT1 functions as a transcriptional regulator and contributes to a cancer-favorable transcriptome, thereby promoting tumorigenesis in experimental animal models. Our analysis of the transcriptional role of NEAT1 identified functions beyond its previously speculated role in maintaining the integrity of subnuclear organelles called paraspeckles[5]. We demonstrate that NEAT1 is recruited to the chromatin of well characterized prostate cancer genes and contributes to an epigenetic “on” state. Analysis of two large clinical cohorts nominated NEAT1 as a novel biomarker of disease progression. Given its significance within the ERα signaling pathway, we propose that targeting NEAT1 might represent a novel and important therapeutic strategy for the treatment of prostate cancer.

RESULTS

ERα in transcriptional regulation of prostate cancer

To elucidate the role of ERα in prostate cancer, we analyzed ERα protein and transcript levels in a panel of prostate cancer cell lines (n=5) and in a cohort of matched benign prostate tissue (n=14) and prostate adenocarcinoma (PCa) (n=14), respectively. We observed that ERα was significantly upregulated (p=0.03) in prostate tumors compared with benign tissues (**Fig. 1a**). To determine the clinical relevance of ERα in prostate cancer, we performed immunohistochemistry using a tissue microarray composed of tissue cores from 64 samples of benign prostate tissue, 16 high-grade prostate intraepithelial neoplasia (HGPIN), 292 PCa, and 42 neuroendocrine prostate cancer (NEPC). Representative photomicrographs are depicted in **Supplementary Fig. 1a**. While benign prostate had only low expression levels of ERα, ERα was detected in adenocarcinoma and the adjacent HGPIN through focal nuclear and cytoplasmic staining (**Supplementary Fig. 1a**). ERα is overexpressed in a significant number of prostate cancer cohorts. It was also found to be overexpressed in prostate cancers with high Gleason score compared to those with low Gleason score as well as in those with tumor recurrence when analyzed via the Oncomine[6] database (**Fig. 1b**)[7-22]. Analysis of subcellular distribution in prostate cancer cell lines revealed significant nuclear distribution of ERα in all cell lines tested (**Supplementary Fig. 1b**). ERα protein levels were similar in both AR-positive LnCaP and VCaP cells (**Fig. 1a, inset**). We used parental VCaP and the ERα-positive prostate cancer cell line NCI-H660 as model cell lines to further explore and delineate the specific contribution of ERα to prostate cancer. A ligand-dependent modulation of invasive potential was observed in VCaP cells

upon estrogen (E2) treatment (**Fig. 1c**). These results suggest that a functionally relevant, ligand-dependent ERα signaling pathway is active in prostate cancer cell lines.

To further understand the impact of ERα, we generated VCaP cells that overexpress ERα (VCaP ERα). Stable expression of ERα was confirmed by Western blot (**Supplementary Fig. 1c**). VCaP ERα exhibited significantly higher invasive potential than VCaP parental cells or the vector control cells (**Fig. 1c**). Intriguingly, the noted effects of ERα overexpression were independent of AR status, as experimental silencing of AR in VCaP ERα cells (**Supplementary Fig. 1c**) did not compromise the increased invasive potential of E2-treated VCaP ERα cells (**Fig. 1c**). These data suggest that prostate cancer cells can utilize alternate nuclear receptor signaling (e.g., ERα signaling) to propagate, and understanding these mechanisms will help discern the complete spectrum of key regulators of prostate cancer progression.

Studies have established ERα's dominant role in transcriptional regulation of target genes in breast cancer[23,24]. Likewise, high nuclear levels of ERα in prostate cancer cells (**Supplementary Fig. 1b**) and their direct association with chromatin implicate ERα in the transcriptional regulation of this cancer, as well. We used ERα chromatin immunoprecipitation coupled with high-throughput sequencing (ChIP-seq) in VCaP cells, with and without E2 treatment, and also in VCaP ERα and NCI-H660 cells with E2 treatment to investigate the underlying mechanisms by which ERα might drive a transcriptional program in prostate cancer. The majority of ERα-binding sites were cell-specific (**Supplementary Fig. 1d**). Analysis of the ChIP-seq data for ERα in NCI-H660 and VCaP ERα cells revealed that 64.9% of ERα binding occurred within intergenic regions of the prostate genome. This fraction is higher than the expected fraction if peaks were randomly distributed across the genome (p=3e-05) (**Supplementary Fig. 1e**).

Using publicly available datasets[25], we found that 28% of the intergenic ERα binding sites in the prostate cancer genome (from VCaP ERα and NCI-H660 cell lines) overlapped with the active histone marks tri-methylated lysine 4 of histone H3 (H3K4me3) and tri-methylated lysine 36 of histone H3 (H3K36me3) (p<1e-7). On the other hand, 20.7% of those sites overlapped with histone marks typical of inactive chromatin, such as tri-methylated lysine 9 of histone H3 (H3K9me3) or tri-methylated lysine 27 of histone H3 (H3K27me3). To prioritize experimental validation of ERα targets, we ranked the peaks according to the average p-value determined by the peak-calling algorithm ChIPSeeqer[26] and selected the highest ranking peaks for further analysis. We analyzed recruitment of endogenous ERα to the top 11 binding sites in parental VCaP cells (**Fig. 1d**) providing an experimental validation of the ChIP-seq data. A significantly higher recruitment of ERα was evident at the binding sites compared to control IgG.

Given the enhanced recruitment of ERα to intergenic regions in the prostate genome, we evaluated the likelihood that ERα might influence transcriptional output and thereby the repertoire of non-coding RNA in the context of prostate cancer. We thus analyzed the abundance of non-coding transcripts in RNA-seq data derived from a cohort of 73 prostate tissues which included 26 benign prostate samples, 40 PCa, and 7 NEPC (**Supplementary dataset 1**), focusing our analysis on 6,850 intergenic lncRNAs out of 12,143 known

lncRNAs (**see Supplementary methods).** We identified 1,314 and 1,399 intergenic lncRNAs that are differentially expressed between benign and PCa and between PCa and NEPC, respectively (FDR < 0.01). We identified 140 intergenic lncRNAs putatively regulated by ERα (**Fig. 1e** and **Supplementary dataset 2**). An analysis of AR binding sites[25] identified 98 lncRNAs that have an AR binding site within the promoter. This supported the view that ERα might significantly influence the non-coding transcriptome in prostate cancer. Using the RNA-seq data on VCaP and VCaP ERα cell lines to validate the expression levels of the top differentially expressed ERα-regulated lncRNAs, we selected six potential candidate lncRNAs that had higher expression in VCaP ERα compared with VCaP. We used quantitative real-time PCR (qRT-PCR) to validate expression for these six ERα regulated lncRNAs in VCaP and VCaP ERα-expressing cell lines (**Supplementary Fig. 1f**). Expression of three of these lncRNAs was further determined in a cohort of 28 matched benign and prostate cancer samples, confirming upregulation of these three nominated lncRNAs in prostate cancer compared with benign prostate (**Fig. 1f**). Taken together, these analyses indicate that ERα is a transcriptional regulator of the non-coding transcriptome in prostate cancer.

Among the putatively ERα-regulated intergenic lncRNAs, we identified Nuclear Enriched Abundant Transcript 1 (NEAT1) as the most significantly overexpressed lncRNA in prostate cancer versus benign prostate in our patient cohort (73 samples) (**Fig. 1f; Supplementary dataset 2**). The NEAT1 gene is located on chromosome 11q13.1 and produces two RNA isoforms that overlap completely at the 5' end. The shorter isoform (hereafter abbreviated as NEAT1/NEAT1_1) is 3.7kb in length and more abundant than the longer, 23kb isoform (NEAT1_2)[27]. NEAT1 lncRNA is essential for the formation of subnuclear bodies called paraspeckles[27], and while both isoforms localize to paraspeckles, their physiological role in prostate cancer remains unknown.

ERα-regulated NEAT1 lncRNA is upregulated in prostate cancer

In the Oncomine database, we observed significant overexpression of NEAT1 lncRNA in several prostate cancer datasets (normal vs. cancer) and aggressive prostate cancer (**Fig. 2a**)[7,10-22,28-31]. We first confirmed that amplification of chromosome 11q (where NEAT1 resides) was not seen across 109 adenocarcinoma cases[32], eliminating chromosome 11q13.1 amplification as an explanation for high NEAT1 expression (**Supplementary Fig. 2a**)[33,34]. The expression of NEAT1 in two radical prostatectomy cohorts with long-term clinical follow-up from the Mayo Clinic[35,36] was measured using Affymetrix HuEx microarrays (see Methods). **Supplementary Table 1** contains the patient characteristics of the datasets. NEAT1's expression ranked in the 99th percentile of all genes on the microarray (**Fig. 2b**). We determined levels of NEAT1 by RNA *in situ* hybridization (ISH) in a tissue microarray that included 16 benign prostate tissues, 21 PCa, 12 PCa with neuroendocrine differentiation, and 7 NEPC cases. NEAT1 was found to be highly expressed in prostate cancer compared with benign tissue (**Supplementary Fig. 2b**).

We observed that in a panel of prostate cancer cell lines ERα overexpression and E2 treatment upregulated NEAT1 transcript levels in a time-dependent manner (**Fig. 2c**). In DU145, an ERG-negative cell line[37], E2/ERα signaling was intact (**Fig. 2c**), supporting an

ERG-independent phenomenon. Following ERα overexpression we recorded an increase in expression of the long isoform NEAT1_2, but to a lesser extent than the short form (**Supplementary Fig. 2c**). This was not surprising as both isoforms of NEAT1 are driven by the same promoter[38]. The preferential upregulation and increase in the NEAT1 long form alone is not well understood and is not further addressed in this study. Interestingly, knockdown of ER beta (ERβ) did not alter NEAT1 levels, suggesting that NEAT1 regulation is specific for ERα (**Supplementary Fig. 2d**).

NEAT1 was originally identified with subnuclear organelles called paraspeckles that are free of chromatin and function as repositories of edited RNA and a number of nuclear RNA-binding proteins[5]. Loss of NEAT1 dramatically reduces the formation of paraspeckles. Treatment of the VCaP cells with E2 resulted in re-distribution of NEAT1 from paraspeckles to an enhanced distribution throughout the nucleus (**Supplementary Fig. 2e**).

We inspected our ERα ChIP-seq data in VCaP ERα and NCI-H660 cells and identified two ERα binding sites on the NEAT1 promoter (**Fig. 2d**). Analysis of chromatin marks using ChIP-seq data sets for histone marks[25] revealed the presence of active histone marks H3 Acetyl K9 and H3K4me3 in the promoter region of NEAT1, while H3K36Me3 marks were abundant in the gene body (**Fig. 2d**). A recent study revealed that bivalent H3K4Me3 and H3K36Me3 marks are indicators of functional transcriptional loci from the non-coding genome[39]. ERα recruitment to specific regions of the NEAT1 promoter was independently validated by ERα ChIP in VCaP, VCaP ERα and NCI-H660 cells (**Figs. 2e, and Supplementary Fig. 2f & 2g**) using specific primers encompassing ERα binding sites in the NEAT1 promoter. We found that a functional estrogen/ERα signaling pathway was active in VCaP cells, as determined by reporter-based ERE luciferase assays in VCaP cells, with ERα and AR overexpression and E2 or R1881 treatment respectively for 48 h (**Fig. 2f**). To further test whether ERα is required for NEAT1 transcriptional activation, we generated luciferase promoter reporter constructs with both ERα binding sites upstream of the luciferase-coding region. Luciferase reporter assays in VCaP cells confirmed that NEAT1 promoter activity was upregulated in an ERα-dependent manner and further enhanced with E2 treatment (**Fig. 2g**).

ERα and NEAT1 regulate several prostate cancer genes

We next sought to understand the physiological role of NEAT1 and to determine the downstream targets of the ERα-NEAT1 axis in prostate cancer. We were particularly interested in identifying genes significantly deregulated in prostate cancer and positively correlated with ERα and NEAT1 expression. Transcriptome sequencing of VCaP and VCaP ERα cells and pairwise comparison revealed 588 genes to be upregulated in VCaP ERα cells (log2 fold change > 2) (**Supplementary dataset 3, Fig. 3a**). We performed a comparative analysis of this 588-gene signature using Oncomine concept analysis. We focused on datasets from prostate cancer studies that included both prostate tumor and benign prostate tissues. The analysis revealed that the ERα gene signature was significantly upregulated in a number of prostate cancer datasets, but was downregulated in other non-prostate datasets, indicating that ERα regulates prostate cancer-specific genes (**Fig. 3b, Supplementary Table 2**).

To validate if ERα targets identified by *in silico* analysis are dependent on cellular levels of ERα, we experimentally silenced ERα in VCaP cells using an siRNA approach and determined transcript levels of 10 target genes using qRT-PCR. The target genes selected for validation were those genes that demonstrated the highest log2 fold difference in VCaP and VCaP ERα cells. Results indicated that mRNA levels of the target genes selected were dependent on ERα (**Fig. 3c**), suggesting a distinct contribution of ERα in determining the transcriptional program.

NEAT1 is a downstream target in the ERα signaling pathway

After determining an ERα signature, we next investigated the potential role of NEAT1. Interestingly, knockout of NEAT1 compromised the expression of ERα target genes, suggesting that NEAT1 is not only a downstream target but also a mediator of ERα signaling in prostate cancer cells (**Fig. 3d**). To evaluate this further and to determine if a functional synergy between ERα and NEAT1 pathways exists in prostate cancer cells, we performed RNA-seq of vector control and NEAT1-overexpressing VCaP cells to determine a NEAT1 signature. To achieve this we limited our analysis to genes that were upregulated four-fold in NEAT1-expressing cells (**Supplementary dataset 4**). Interestingly NEAT1 signature showed a strong correlation with the ERα signature genes (q=1.90E-120). Analysis of the top 1000 genes of the NEAT1 signature revealed that this signature is upregulated in prostate cancer datasets when compared with other cancer datasets (**Fig. 3e, Supplementary Table 2**). Furthermore, NEAT1 signature was also upregulated in all prostate cancer datasets (comparing benign vs. PCa; odds ratio > 2.0 and $P < 1 \times 10^{-6}$) (**Supplementary Fig. 3a**).

We also queried Oncomine prostate datasets to identify genes whose mRNA levels correlate with those of NEAT1 (correlation coefficient > 0.5). We compared this gene list with the ERα signature genes from our analysis in **Fig. 3a** and identified 155 genes in common. These 155-gene were also found to be upregulated in all prostate cancer datasets compared with other cancer datasets (only normal vs. cancer datasets were considered; odds ratio > 3.0 and $P < 1 \times 10^{-6}$) (**Supplementary Table 2 & Supplementary Fig. 3b**).

To determine if the genes identified by *in silico* analysis are indeed influenced by NEAT1, we silenced NEAT1 in VCaP cells and determined transcript levels of potential target genes using qRT-PCR. We selected the top 10 genes that were significantly correlated to NEAT1 expression across all prostate cancer concepts. As expected, mRNA levels of these selected target genes were indeed dependent on NEAT1, further confirming a definite role of NEAT1 in the transcriptional program (**Fig. 4a**). In addition to cell lines, we also determined transcript levels of these ERα-NEAT1 signature-selected genes in a small patient cohort (n=26) of 13 matched benign and prostate adenocarcinoma, respectively. We observed that relative mRNA levels of these NEAT1-ERα signature-selected genes revealed significant upregulation in prostate cancer (**Fig. 4b**). We computed the log2 fold change of expression levels using the 13 paired tumor/benign samples for NEAT1 and for these selected genes. We then correlated the fold change values, and observed a moderate to strong correlation between NEAT1 and the associated genes in clinical samples (**Fig. 4c**). Among these seven genes, prostate-specific membrane antigen (*PSMA*) and alpha-methylacyl-CoA racemase

(*AMACR)* are well-known diagnostic and, in the case of PSMA, prognostic markers of prostate cancer progression[40-44]. Furthermore, knocking down ERβ did not alter expression of key signature genes in LnCaP, PC3, VCaP and NCI-H660 cells (**Supplementary Fig. 3c**), suggesting a non-redundant regulatory role for ERα.

NEAT1 and chromatin regulation

To study the potential role of NEAT1 in regulation of target genes *in vivo* we performed luciferase reporter assays using PSMA-luc as a candidate NEAT1 target. NEAT1 induced robust activation of the *PSMA* promoter in PC3 cells (**Fig. 5a**) and VCaP cells (**Fig. 5b**). These results prompted us to investigate if NEAT1 is recruited to chromatin of target genes. We used the ChIRP approach[45] to pull down endogenous NEAT1 from VCaP cells. Analysis of the ChIRP data revealed that NEAT1 is recruited to the *PSMA* promoter, but not the downstream exon 1 (**Fig. 5c**). In addition to *PSMA*, we also tested NEAT1 recruitment to other target genes described in **Fig. 3c** and **Fig. 4a** and observed that in addition to *PSMA*, NEAT1 was also recruited to the promoter region of *GJB1* (**Supplementary Fig. 4a**). This suggests that NEAT1 transcriptionally regulates a compendium of genes known to be involved in prostate cancer progression. We hypothesized that NEAT1 might contribute to gene transcription by interacting with chromatin-modifying proteins and/or interacting with histones. Several recent studies support the view that lncRNAs recruit chromatin-modifying machinery[46-49]. To test this hypothesis, we analyzed the chromatin landscape at the *PSMA* promoter and observed that NEAT1_1, and not NEAT1_2, facilitated gene transcription by promoting an active chromatin state (**Fig. 5d**). Overexpression of NEAT1_1 significantly increased active chromatin marks at the *PSMA* promoter (i.e., H3K4Me3 and H3AcK9). Of note, ERα was not significantly recruited to the *PSMA* promoter when expressed alone. Overexpression of NEAT1_1 resulted in subsequent recruitment of NEAT1_1 and ERα to the *PSMA* promoter. These studies indicate that while NEAT1_1 may function as a chaperone for ERα and other chromatin-modifying machinery to target promoters, binding of ERα and/or recruitment to NEAT1_1 targets is not necessary for transcriptional activation.

As our data suggest that NEAT1 overexpression favors a chromatin landscape for active transcription, we investigated whether NEAT1 could directly interact with nucleosomal histones. Nuclear lysates from VCaP cells were used in an immunoprecipitation experiment with streptavidin-beads coupled with either scrambled, antisense NEAT1, or antisense NR_024490 (another ERα lncRNA target) oligonucleotides. NEAT1 was found to specifically associate with histone H3 (**Fig. 5e, left panel, lane 8**) and the specificity of this binding is apparent when comparing lanes 7 and 9, which represent Streptatividin-IP using scrambled biotinylated oligos and Streptavidin-IP using antisense-NEAT1 oligos and nuclear lysates from NEAT1 siRNA treated cells, respectively. As an additional negative control, we used scrambled and specific antisense oligos for a different lncRNA, NR_024490, another ERα target. The results indicate that NEAT1 can associate with chromatin via specific interaction with histone H3. We also determined association of NEAT1 with active histone H3 modifications, including H3AcK9 and H3K4Me3 (**Fig. 5e, right panel**). Similar association patterns were seen for NEAT1 in NCI-H660 cells (**Supplementary Fig. 4b**).

To complement this finding, we performed RNA immunoprecipitation from VCaP ERα cells using anti-histone H3 and anti SNRNP70 (positive control) as the immunoprecipitating antibody. qRT-PCR showed robust binding of NEAT1 to histone H3 (**Supplementary Fig. 4c**). The positive control U1 snRNA showed high enrichment in the immunoprecipitate with SNRNP70. To further confirm the specificity of NEAT1 binding to histone H3, we performed a streptavidin-biotin pull down assay in VCaP and VCaP ERα cells with and without E2 (**Supplementary Fig. 4d**). These data suggest that NEAT1 can directly interact with the histone H3 component of chromatin.

NEAT1 promotes prostate tumorigenesis

To better understand the physiological role of NEAT1 in context of ERα in prostate cancer, we first determined levels of NEAT1 in VCaP cells overexpressing ERα (**Supplementary Fig. 5a)**. Further, we generated stable VCaP and VCaP ERα cell lines that overexpress NEAT1 (**Supplementary Fig. 5b**). We also knocked down NEAT1 in VCaP and VCaP ERα-expressing cells by stably expressing NEAT1 shRNA targeting two different regions of NEAT1 and non-targeting shRNA (**Supplementary Fig. 5c**). While overexpression of NEAT1 significantly increased proliferation and cell invasion, knockdown of NEAT1 significantly decreased proliferation and the invasive properties of the cells (**Figs. 6a & 6b**).

Soft agar assays were performed in both VCaP and VCaP NEAT1 cells. Colonies were monitored over a period of 21 days. Overexpression of NEAT1 resulted in a significantly higher number of viable colonies (**Fig. 6c**). Colony-forming assays performed in NEAT1 clones in VCaP cells with and without E2 demonstrated that E2 treatment in NEAT1-overexpressing cells significantly increased the number of colonies (**Fig. 6d**). These *in vitro* assays establish an oncogenic role for NEAT1.

To further validate the oncogenic role of NEAT1, we extended our studies to an *in vivo* model system. We performed xenograft studies in NOD-SCID mice. The mice were treated with time-release estrogen pellets. They were divided into two groups and one group was implanted subcutaneously with VCaP ERα cells expressing control shRNA and luciferase reporter and the other group with VCaP ERα cells expressing NEAT1 shRNA luciferase reporter. The mice from both groups were imaged weekly for luciferase activity and **Fig. 6e** shows the bioluminescent signals at day 7 and day 35. The tumor growth was monitored weekly for 45 days and was found to be significantly lower in the NEAT1 shRNA-expressing group compared with the control group (**Fig. 6f**). The tumors were excised and weighed and the NEAT1 shRNA group had significantly smaller tumors (**Supplementary Fig. 6a & b**). We confirmed the efficacy of the shRNA *in vivo* by measuring the NEAT1 and ERα levels in the tumors (**Supplementary Fig. S6c**).

To further substantiate our hypothesis that NEAT1 plays a role in tumorigenesis, we repeated the experiment in athymic nude mice using VCaP control and VCaP NEAT1-overexpressing cells as well as NCI-H660 and NCI-H660 NEAT1-overexpressing cells. In both these experiments, a significantly higher tumor growth was seen in the NEAT1-overexpressing cells (**Figs. 6g & h, Supplementary Figs. 6d & e**) further confirming its oncogenic potential. qRT-PCR analysis confirmed an increased expression of the NEAT1

signature genes in VCaP NEAT1 xenografts compared with control VCaP xenograft tissue (**Supplementary Fig. 6f**).

NEAT1 is associated with therapeutic resistance

Studies presented so far show that ERα establishes an oncogenic cascade and that NEAT1 functions as a downstream mediator of ERα signaling. The ERα- NEAT1 axis is functional both in AR-positive and -negative cell lines and drives prostate carcinogenesis. We hypothesized that targeting NEAT1 using mechanisms that can constrain ERα might represent a novel therapeutic strategy in prostate tumors that are resistant to anti-androgen therapy. To test this hypothesis *in vitro* we evaluated the effect of anti-estrogens and anti-androgens on NEAT1 levels in prostate cancer cell lines. As shown in **Fig. 7a & b,** NEAT1 expression is constrained when cells are treated with the ERα antagonists ICI 182,720 (ICI) and 4-hydroxy tamoxifen (4OHT) in combination with E2. Intriguingly, treatment of ICI and 4OHT alone for longer periods can enhance NEAT1 expression (**Fig. 7a & b**). We observed similar results with AR antagonists enzalutamide and bicalutamide (**Fig. 7c & d**). These results provide compelling evidence to evaluate NEAT1 levels in advanced CRPC cases. RNA-FISH analysis of benign and advanced prostate tumors, including CRPC and NEPC tumor tissue samples illustrated significantly upregulated NEAT1 levels in advanced prostate cancer, with enhanced focal staining throughout the tumor tissue (**Fig. 7e**). We also screened 9 cases of benign prostate, 7 PCa, and 7 CRPC (**Supplementary Table 3**) for NEAT1 and ERα expression by qPCR (**Fig. 7f**), and both NEAT1 and ERα levels were significantly higher in the CRPCs. We determined the correlation between NEAT1 and ERα expression by estimating the Pearson's correlation coefficient R. The results indicate a strong positive correlation: R = 0.86 (p-value=1.9e-07). Taken together, our results present a novel role for the non-coding transcriptome in cancer-favorable adaptations.

NEAT1 is associated with aggressive prostate cancer

Given the importance of NEAT1 in promoting tumorigenesis both *in vitro* and *in vivo*, we sought to determine the relationship between NEAT1 levels and prostate cancer clinical outcomes in 594 patients from two radical prostatectomy cohorts with long-term clinical follow-up from the Mayo Clinic[35,36]. **Supplementary Table 1** contains the patient characteristics of men who underwent radical prostatectomy at the Mayo Clinic Comprehensive Cancer Center between 1987 and 2001 for clinically localized prostate cancer.

We assessed the prognostic potential of NEAT1 expression using several statistical measures and correlating it with biochemical recurrence (BCR) and metastasis (MET), prostate cancer-specific mortality (PCSM) and Gleason score (GS) > 7. In order to evaluate endpoints of disease aggressiveness and progression based on NEAT1 expression, Kaplan-Meier (KM) analysis was performed for the BCR and MET endpoints. The resulting KM curves (**Figs. 8a & b**) demonstrate that patients with higher NEAT1 expression have significantly worse outcomes for both BCR (p-value: 0.028) and MET events (p-value: 0.016).

Patient risk discrimination based on the expression profile of NEAT1 was assessed by area under the receiver operating characteristic curve (AUC) with 95% confidence intervals (CI), (**Supplementary Fig. 7**). NEAT1 significantly segregates patients who exhibited BCR, MET, PCSM and GS > 7.

To further compare NEAT1's prognostic ability to other clinicopathologic variables, univariable odds ratios were computed for the BCR, MET, PCSM, and GS > 7 endpoints (**Fig. 9**). NEAT1 was significantly prognostic for segregating high-risk from low-risk patients for each of the endpoints ($p<0.05$). Further multivariate analysis adjusting for adjuvant radiation and hormone treatment, in addition to the other clinicopathological variables assessed, also demonstrates that NEAT1 was significantly prognostic for BCR, MET, and GS>7, supporting NEAT1 as a prognostic biomarker for aggressive prostate cancer independent of common clinical and pathologic variables (**Supplementary Fig. 8**). Overall, these results show that NEAT1 is significantly prognostic for several clinically relevant endpoints.

DISCUSSION

The tissue-specific role of ERα in breast and other gynecological malignancies is well understood. Interestingly, ERα is expressed in all prostate cancers, including those that lack AR expression, while it is absent in normal prostate epithelium. Studies from our and other laboratories have examined the relevance of ERα in prostate cancer[4,50-52]. ERα-mediated regulation of oncogenic TMPRSS2-ERG fusion and estrogen regulation of the *EBAG9* gene, that confirms aggressive behavior of prostate cancer, are noted examples that suggest a functional ERα-signaling pathway exists in prostate cancer. From a clinical perspective, the association of a polymorphism in ERα with prostate cancer with a favorable Gleason score or cancers of late onset has also been reported[53]. These initial observations prompted us to evaluate if re-expression of ERα, and the establishment of an alternate nuclear receptor-signaling axis (i.e., ERα versus AR), in prostate cancer cells could represent an adaptive mechanism to evade AR-directed therapies.

Analysis of global ERα recruitment in prostate cancer cells using a ChIP-seq approach revealed that ERα is preferentially recruited to intergenic regions of the prostate genome. Comparison of binding profiles with transcriptome sequencing data suggested that ERα drives expression of non-coding transcripts. These results led us to analyze the functional consequences of ERα recruitment to non-coding regions. From a large compendium of ERα-regulated non coding transcripts, we selected NEAT1 for a detailed biochemical and *in vivo* evaluation, based on an *in silico* approach that demonstrated a strong association of NEAT1 with prostate cancer progression. We show that ERα transcriptionally regulates NEAT1. NEAT1 is recruited to the promoter of several key target genes and induces an active chromatin state favorable for transcription. Our studies indicate that ERα does not function as a molecular chaperone to guide NEAT1 to target chromatin; rather, we suspect that a complex proteome of chromatin-interacting proteins interacts with and guides NEAT1 to promoter targets. Interestingly, both ERα and NEAT1 signaling were refractory to AR inhibitors and the lack of AR or ERβ, thus indicating a functional specialization of the ERα-NEAT1 axis for prostate cancer progression. Furthermore, introduction of cells

overexpressing NEAT1 could clearly induce prostate cancer progression in experimental animal models.

The current study opens up a new arena of alternative mechanisms of tumorigenesis by ERα in prostate cancer. We show ERα regulates NEAT1 lncRNA with distinct chromatin regulatory functions. Large-scale bioinformatic analysis of SAGE libraries has identified NEAT1 as one of the differentially regulated lncRNAs between some types of cancer and normal tissue[54]. However, its possible role in promoting tumorigenesis has never been explored. We show here that NEAT1 regulates expression of prostate cancer genes by altering the epigenetic landscape at target gene promoters to favor transcription. A closer examination of NEAT1 revealed a previously uncharacterized role in recognition of modified histones. We have not tested if NEAT1 is a reader of multiple histone H3 post-translational modifications (acetylation, methylation, etc.), and our laboratory is actively pursuing this intriguing question. NEAT1 expression independently was sufficient to activate prostate cancer genes in an AR independent manner. Further, our results confirmed an oncogenic role for NEAT1 in an experimental animal model of prostate cancer and in cell culture models.

Molecular sieving of net non-coding transcriptome using comprehensive bioinformatic approaches and wet-lab validation over a decade has indicated that the non-coding transcriptome has a regulatory role beyond the speculated “transcriptional noise” and a direct influence on the coding transcriptome and biologic homeostasis. We observed that several lncRNAs like NEAT1 respond to cellular cues and ligand signaling in a manner reminiscent of the coding transcriptome. Thus far the literature on NEAT1 has focused on its architectural role in forming subnuclear paraspeckles[27]. Our results indicate a role for NEAT1 beyond that of paraspeckles. It would be interesting in the future to reconcile how the formation of paraspeckles in the inter-chromosomal space ties in with the role of NEAT1 in activating gene expression at promoters. Our lab continues to pursue some of these unanswered questions in order to better understand the role of NEAT1.

Our identification of an ERα-NEAT1 axis illustrates a mechanism whereby prostate cancer cells may develop therapeutic resistance through positive selection of an alternate nuclear receptor signaling pathway in the absence of AR or during androgen ablation therapy (**Fig. 10**). However, we cannot exclude the presence of other NEAT1-interacting chromatin factors. This is the subject of ongoing investigation. From a clinical perspective our studies indicate for the first time that NEAT1 is significantly prognostic for several clinically relevant endpoints. In prostatectomy specimens from two large cohorts, high NEAT1 expression was associated with a significant increase in both biochemical and metastatic recurrence rates compared to those with low NEAT1 expression.

In summary, this study provides important insights into a unique mechanism of ERα regulation in prostate cancer and identifies NEAT1 as a novel prognostic marker and potential therapeutic target in this disease. While our studies have identified a previously unexplored function of ERα in regulating lncRNAs, it is also the first of its kind to demonstrate transcriptional regulation of lncRNAs by an alternative steroid receptor in prostate cancer. We propose that NEAT1 is directly involved in modulation of the

phenotype of a leading disease. Combinatorial targeting of NEAT1 and AR may represent a unique therapeutic regimen within a subset of patients with advanced prostate cancer.

METHODS

Cell culture and treatments

LnCaP and PC3 cells were grown in RPMI 1640 (Invitrogen) and supplemented with 10% fetal bovine serum (FBS) and 1% penicillin-streptomycin. RWPE1 cells were grown in Keratinocyte Serum Free Medium (K-SFM), Kit (Gibco, #17005-042). VCaP and DU145 cells were grown in DMEM (Invitrogen) and supplemented with 10% fetal bovine serum (FBS) with 1% penicillin streptomycin. NCIH660 cells were grown in RPMI 1640 supplemented with 0.005 mg/ml insulin, 0.01 mg/ml transferrin, 30 nM sodium selenite, 10 nM hydrocortisone, 10 nM β-estradiol, 5% FBS, 1% penicillin-streptomycin and an extra 2 mM of L-glutamine (for a final concentration of 4 mM). For cell treatments in several experiments, we used 10-100 nM β-estradiol (Sigma Aldrich), 10μM Enzalutamide (Astellas), 10μM bicalutamide (Sigma Aldrich), 1-10nM R1881 (PE Biosystems), 10-100 nM 4-hydroxy tamoxifen (4OHT) (Sigma Aldrich), 1-10μM ICI 182,720 (Tocris Bioscience).

Plasmids, siRNAs and transfection

pcDNA 3.1, pcDNA3.1-ERα, pcDNA 3.1 AR, piLenti-GFP, piLenti-NEAT1 siRNA-GFP (set of four, sequences provided in **Supplementary Table 4**), iLenti-si-scrambled, pLenti-bicistronic-luc-NEAT1. siRNAs for ERα, ERβ, AR, NEAT1, NEAT1_2 were used and the sequence is provided in **Supplementary Table 4**. For the mammalian expression vectors Lipofectamine 3000 (Invitrogen) and Lonza nucleofection were used for transfection. The stable clones for NEAT1 overexpression as well as the scrambled and NEAT1 shRNA expressing cells were generated by using the lentiviral vectors and by selection in puromycin.

Identification of ERα-regulated lncRNA

A set of known lncRNAs was generated from various data sources: RefSeq: GENCODE v7; - ncRNA.org; and lncRNAdb[55] (see **Supplementary material**) and those that were at least 200nt long were selected, resulting in 12,483 lncRNAs. These lncRNAs were characterized according to their potential of being regulated by ERα by using ERα binding sites information from ChIP-seq experimental data. Moreover, several histone marks were considered to provide evidence of transcription, including H3K4me3 and H3K36me3 (details in **Supplementary material**).

Differential expression analysis

In order to prioritize the experimental validation of lncRNAs, a pair-wise differential expression analysis was performed on the expression values determined by paired-end transcriptome sequencing of 73 samples (26 benign prostate, 40 PCa, and 7 NEPC). A pair-wise Wilcoxon test was performed and all p-values were corrected for multiple hypotheses testing using Benjamini-Hochberg[56] (details in **Supplementary material**).

ERα and NEAT1 signature via Oncomine concept analysis

RNA sequencing was done for VCaP and VCaP ERα-expressing cells as well as in vector control and NEAT1 overexpressing VCaP cells (detailed in **Supplementary methods**). The expression of the genes was computed and those genes with a log2-fold change greater than 2 were selected. Results are reported in **Supplementary datasets 3 & 4**. 588 genes were found to be overexpressed in VCaP ERα cells. A custom concept of this gene list was generated in Oncomine (**Supplementary Table 2)**. Similarly, genes from the VCaP NEAT1 group with a log2-fold change greater than 2 were selected and a custom concept was built in Oncomine using the top 1000 genes from NEAT1 signature (**Supplementary Table 2)**. The significantly associated tumor vs. normal concepts with odds ratio > 2.0 and $P < 1 \times 10^{-6}$ considering tumor vs. normal analysis was determined. The resulting concepts and associations are represented through a concept network using Cytoscape version 2.8.2. Each node represents a concept to which the signature is associated at a greater than 3-fold odds-ratio for ERα signature and >2 fold odds ratio for NEAT1 signature. Node size reflects the concept size, i.e. the number of genes in each concept; red and green colors represent correlation with over- or under-expressed genes in the concept, respectively; and edge thickness represents the odds- ratio of the association between concepts, ranging from 1.4 to 29.9 and 1.2 to 637 for ERα and NEAT1 signatures, respectively. The border color of each node represents the tumor type. The layout of the network is based on the Edge-weighted spring-embedded algorithm.

Luciferase reporter assays

For ERE luciferase assays, VCaP cells were transiently transfected with the (ERE)3-SV40-luc reporter plasmid and/or ERα and/or AR as well as an internal control construct pRL harboring the renilla luciferase gene. VCaP cells were also transfected with empty vector or NEAT1 promoter (1+2) luciferase reporter constructs alone or with ERα as well as an internal control construct pRL harboring renilla luciferase gene. In order to determine the PSMA reporter activity, 293T cells and PC3 cells were co transfected with empty vector or PSMA luc and Renilla-luc reporter genes alone or with NEAT1, NEAT1 + ERα, or NEAT1 + AR.

24h post transfection the media was changed to 5% charcoal stripped media and the cells indicated were treated with E2 (10nM) or R1881 (1nM) for 14h. At 48h cells were lysed with passive lysis buffer and luciferase activities were measured using the dual luciferase system (#E1910, Promega) and normalized with renilla luciferase activity.

RNA *in situ* hybridization for NEAT1

RNA ISH for NEAT1 was performed on 5 benign, 5 PCa and 3 CRPC cases using kits and probes designed by Advanced Cell Diagnostics. Briefly, the single-color chromogenic detection assay uses pairs of specially designed oligonucleotide probes that, through sequence-specific hybridization, recognize both the specific target NEAT1 RNA sequence and the signal amplification system. Unique target probe oligonucleotides were designed to hybridize in tandem to the target RNA. Cross-hybridization to other sequences is minimized by screening against the entire human RNA sequence database.

The signal amplification system consists of the preamplifier, amplifier, and enzyme-conjugated label probe, which assemble into a tree-like complex through sequential hybridization. Signal amplification occurs at target sites bound by probe pairs only. Nonspecific off-target binding by single probes does not result in signal amplification.

All steps of NEAT1 RNA ISH staining of the slides are performed manually, optimized in tissue microarrays (TMAs). Briefly, formalin-fixed, paraffin-embedded (FFPE) unstained tissue sections (5 μm) were mounted on positively charged microscopic glass slides, deparaffinized in xylene and rehydrated through a series of alcohols. The rehydrated sections were treated with 3% hydrogen peroxide at room temperature for 10 minutes to block endogenous peroxidase. Sections were then boiled in 1× citric buffer (10 nmol/L Nacitrate, pH 6.0) for 15 minutes and incubated with protease (2.5 mg/mL; Sigma Aldrich, St. Louis, MO) at 40°C for 30 minutes. The slides were hybridized sequentially with target probes (20 nmol/L) in hybridization buffer A (6× saline sodium citrate [SSC] buffer [1× SSC is 0.15 mol/L NaCl and 0.015 mol/L Nacitrate], 25% formamide, 0.2% lithium dodecyl sulfate [LDS], and blocking reagents) at 40°C for 2 hours, signal preamplifier in hybridization buffer B (20% formamide, 5×SSC, 0.3% LDS, 10% dextran sulfate, and blocking reagents) at 40°C for 30 minutes, amplifier in hybridization buffer B at 40°C for 30 minutes, and horseradish peroxidase– or alkaline phosphatase–labeled probes in hybridization buffer C (5× SSC, 0.3% LDS, and blocking reagents) at 40°C for 15 minutes.

Hybridization signals were detected under bright field microscope as red colorimetric staining (using Fast Red chromogen, BioCare Biomedical, Concord, CA) followed by counterstaining with hematoxylin. Signals were granular and discrete red signals corresponding to individual lncRNA targets. The signals were scored using the RNA Spot Studio software.

Chromatin immunoprecipitation

All ChIP experiments were carried out using Millipore EZ-Magna ChIP kit (Catalogue # 17-10086). Briefly 5-10 × 10^6 cells were crosslinked with 1% formaldehyde for 10 min at room temperature. The crosslinking was then quenched with 0.125 M glycine. Chromatin was sonicated in the lysis buffer to 300-500 bp and the extraction of ChIP DNA was done as per the kit protocol. Antibodies used include ERα (AC-066-100, diagenode, 5μg), AR (06-680, Millipore, 5μg), H3K4me3 (ab8580, Abcam, 5μg), H3K9me3 (ab8898, Abcam, 5μg), H3K36me3 (ab9050, Abcam, 5μg), H3K27me3 (07-449, Millipore, 5μg), and Ace-H3 (no. 06-599, Millipore, 5μg).

ERα ChIP was also performed in crosslinked VCaP cells with E2 treatment for 0, 14h and 48h. In VCaP ERα cells E2 treatment was for 6h, 14h and 48h. The primer sequences are provided in **Supplementary Table 5**.

Chromatin Isolation by RNA Purification (ChIRP)

Chromatin immunoprecitation for NEAT1 was done in VCaP control and NEAT1 expressing cells with and without E2 treatment using the ChiRP protocol[45]. Briefly, biotin TEG antisense oligos were generated using singlemoleculefish.com for NEAT1, Lac Z and

scrambled NT NEAT1. The NEAT1 probes were divided into 2 pools. Cells cross-linked in 1% gluteraldehyde were lysed and sonicated. The biotinylated probes were hybridized followed by RNA and DNA isolation. qPCR was performed on the DNA samples. Probe sequences are described in **Supplementary Table 6**.

RNA-ISH for NEAT1 on cell lines

Cells were grown on a 15mm, poly-L-lysine coated glass coverslip. At ~70% confluence cells were serum starved in 8% charcoal stripped media for 48h, followed by 48h treatment with 10nM E2. At the end of treatment, cells were fixed in 4% formaldehyde, dehydrated by an ethanol gradient (50-100%) and stored at −20°C. For the hybridization assay cells were rehydrated by an ethanol gradient (100-50%) into PBS. Between subsequent steps cells were washed with PBS. The Affymetrix QuantiGene ViewRNA ISH cell assay kit was used for NEAT1 staining. Cells were permeabilized by 5min incubation at RT in Detergent Solution QC, and digested for 10min at RT by Protease QS (1:4000 in PBS). Then the target specific Probe Set (1:100 in Diluent QF) was allowed to hybridize for 3h at 40±1°C. Between subsequent steps cells were washed by soaking in Wash Buffer. Sequential hybridization steps were conducted for signal amplification—PreAmplifier Mix (1:25 in Diluent QF), Amplifier Mix (1:25 in Diluent QF) and Label Probe Mix (1:25 in Diluent QF) each incubated 30min at 40±1°C. After 2 10min washes in Wash Buffer, nuclei were stained with DAPI and cover slips were mounted to slides with Prolong Gold Antifade Reagent (Life Technologies) for visualization.

Proliferation assay

Cell proliferation was assessed using the CyQUANT NF cell proliferation assay kit (Life Technology). Cells were seeded in 96-well plates at 3-4 × 10^4 cells per well. Cells were incubated in DMEM media with 10% FBS for 24h. The cells were then serum starved in 8% charcoal stripped DMEM medium for 48h followed by E2 treatment at 10nM concentration for indicated time points. The media was then aspirated and replaced with the dye binding solution followed by incubation for 30-60 minutes. The fluorescence was then measured in a microplate reader using excitation at 485 ± 10 nm and fluorescence detection at 530 ± 15 nm. The assay was performed in triplicates.

Invasion assay

The CHEMICON cell invasion assay kit (EMD MIlipore) was used for determining the cell invasion. Cells were serum-starved for 48 hours and then seeded at a density of 2 × 10^5 cells/well in the upper well of the invasion chamber. 500 μl of phenol res free DMEM media supplemented with 8% charcoal stripped serum and 10nM E2 was added to the lower chamber. After 48-hour incubation, the invaded cells were stained by dipping the inserts in the staining solution for 20 minutes. The stained cells were then dissolved in 10% acetic acid and transferred to a 96-well plate for colorimetric reading of OD at 560 nm.

Migration assay

The Cell Biolabs Inc. Radius™ 96-Well Cell Migration Assay was used to determine cell migration. Cells were serum-starved for 48 hours, then seeded to a pretreated (incubated 20

minutes in Radius™ Gel Pretreatment solution and washed with Radius™ Wash Solution) Radius™ 96-Well Plate at a density of 8×10^4 cells per well with or without E2 (10 nM). After 24 hours incubation, the Radius™ Gel Spot was removed via the Radius™ Gel Removal Solution and pre-migration images were captured. After 24 hours incubation, cells were stained with Cell Stain Solution and post-migration images were captured for analysis using the CellProfiler™ Cell Image Analysis Software (Broad Institute).

Statistical analysis

The Wilcoxon test was employed with Benjamini-Hochberg[56] correction for multiple hypotheses for pair-wise comparisons for differential expression analysis. The Chi-square test was used for comparison of proportions and the Pearson's correlation was used to compare the expression of selected genes. For quantitative real time PCR, we computed the Delta CT value according to the ABI qPCR protocol as described in Supplementary methods. To compare qPCR data a student's t-test was employed. Median-rank statistics results are reported for analyses with the Oncomine datasets[57].

Analysis of Mayo Clinic cohort

Affymetrix HuEx microarrays were used to analyze NEAT1 expression in two post-radical prostatectomy cohorts from the Mayo Clinic. Details on tissue preparation, RNA extraction, amplification, hybridization, and clinical characteristics for these cohorts have been described previously[35,36]. Both cohorts were filtered using the same criteria (patient either exhibiting preoperative prostate-specific antigen >20 ng/mL, Gleason score ≥8, pT3b, or GPSM[58] score ≥10) to increase the homogeneity of patient characteristics. The two sets were pooled to improve analytic power, resulting in a dataset of 594 patients. The patient characteristics of the pooled dataset can be found in **Supplementary Table 1**.

A representative Probe Selection Region (PSR) for the genomic span of the short and long NEAT1 isoforms was selected by minimizing the technical variance across the pooled dataset. Based on these two PSRs, the prognostic performance of NEAT1 short and long isoforms was evaluated using univariable and multivariable odds ratios and area under the receiver operating characteristics curve (AUC) for BCR, MET, PCSM, and GS > 7 endpoints. Kaplan Meier (KM) curves were used to perform survival analysis on the Mayo case-cohort patients only[35] since the nested case-control cohort[58] was not suitable for KM analysis.

Supplementary Material

Refer to Web version on PubMed Central for supplementary material.

Acknowledgements

This work was supported by NCI R01 CA152057 (AS, MAR) and the Early Detection Research Network NCI U01 CA111275 (MAR), and the Prostate Cancer Foundation Young Investigator award (DC). We would like to thank Francesca Demichelis for identification of somatic copy number variations, Wasay Hussain for the RNA sequencing analysis, Anastas Popratiloff from George Washington University for helping with immunofluorescence imaging. We would also like to thank John S Mattick and Marcel Dinger for their help in accessing and using data from www.lncrnadb.org. This investigation received editorial support from grant UL1TR000457 of the Clinical and Translation Science Center at Weill Cornell Medical College. This work was supported by NCI R01 CA152057

(AS, MAR) and the Early Detection Research Network NCI U01 CA111275 (MAR), and the Prostate Cancer Foundation (DC, MB).

REFERENCES

1. Heinlein CA, Chang C. Androgen receptor in prostate cancer. Endocr Rev. 2004; 25:276–308. [PubMed: 15082523]
2. de Bono JS, et al. Abiraterone and increased survival in metastatic prostate cancer. N Engl J Med. 2011; 364:1995–2005. doi:10.1056/NEJMoa1014618. [PubMed: 21612468]
3. Scher HI, et al. Increased survival with enzalutamide in prostate cancer after chemotherapy. N Engl J Med. 2012; 367:1187–1197. doi:10.1056/NEJMoa1207506. [PubMed: 22894553]
4. Ricke WA, et al. Prostatic hormonal carcinogenesis is mediated by in situ estrogen production and estrogen receptor alpha signaling. FASEB J. 2008; 22:1512–1520. doi:fj.07-9526com [pii] 10.1096/fj.07-9526com. [PubMed: 18055862]
5. Clemson CM, et al. An architectural role for a nuclear noncoding RNA: NEAT1 RNA is essential for the structure of paraspeckles. Mol Cell. 2009; 33:717–726. doi:S1097-2765(09)00070-7 [pii] 10.1016/j.molcel.2009.01.026. [PubMed: 19217333]
6. Rhodes DR, et al. Oncomine 3.0: genes, pathways, and networks in a collection of 18,000 cancer gene expression profiles. Neoplasia. 2007; 9:166–180. [PubMed: 17356713]
7. Arredouani MS, et al. Identification of the transcription factor single-minded homologue 2 as a potential biomarker and immunotherapy target in prostate cancer. Clin Cancer Res. 2009; 15:5794–5802. doi:10.1158/1078-0432.CCR-09-0911. [PubMed: 19737960]
8. Barwick BG, et al. Prostate cancer genes associated with TMPRSS2-ERG gene fusion and prognostic of biochemical recurrence in multiple cohorts. Br J Cancer. 2010; 102:570–576. doi: 10.1038/sj.bjc.6605519. [PubMed: 20068566]
9. Best CJ, et al. Molecular alterations in primary prostate cancer after androgen ablation therapy. Clin Cancer Res. 2005; 11:6823–6834. doi:10.1158/1078-0432.CCR-05-0585. [PubMed: 16203770]
10. Glinsky GV, Glinskii AB, Stephenson AJ, Hoffman RM, Gerald WL. Gene expression profiling predicts clinical outcome of prostate cancer. J Clin Invest. 2004; 113:913–923. doi:10.1172/JCI20032. [PubMed: 15067324]
11. Grasso CS, et al. The mutational landscape of lethal castration-resistant prostate cancer. Nature. 2012; 487:239–243. doi:10.1038/nature11125. [PubMed: 22722839]
12. Lapointe J, et al. Gene expression profiling identifies clinically relevant subtypes of prostate cancer. Proc Natl Acad Sci U S A. 2004; 101:811–816. doi:10.1073/pnas.0304146101. [PubMed: 14711987]
13. LaTulippe E, et al. Comprehensive gene expression analysis of prostate cancer reveals distinct transcriptional programs associated with metastatic disease. Cancer Res. 2002; 62:4499–4506. [PubMed: 12154061]
14. Liu P, et al. Sex-determining region Y box 4 is a transforming oncogene in human prostate cancer cells. Cancer Res. 2006; 66:4011–4019. doi:10.1158/0008-5472.CAN-05-3055. [PubMed: 16618720]
15. Luo J, et al. Human prostate cancer and benign prostatic hyperplasia: molecular dissection by gene expression profiling. Cancer Res. 2001; 61:4683–4688. [PubMed: 11406537]
16. Singh D, et al. Gene expression correlates of clinical prostate cancer behavior. Cancer Cell. 2002; 1:203–209. [PubMed: 12086878]
17. Taylor BS, et al. Integrative genomic profiling of human prostate cancer. Cancer Cell. 2010; 18:11–22. doi:10.1016/j.ccr.2010.05.026. [PubMed: 20579941]
18. Tomlins SA, et al. Integrative molecular concept modeling of prostate cancer progression. Nat Genet. 2007; 39:41–51. doi:10.1038/ng1935. [PubMed: 17173048]
19. Vanaja DK, Cheville JC, Iturria SJ, Young CY. Transcriptional silencing of zinc finger protein 185 identified by expression profiling is associated with prostate cancer progression. Cancer Res. 2003; 63:3877–3882. [PubMed: 12873976]

20. Varambally S, et al. Integrative genomic and proteomic analysis of prostate cancer reveals signatures of metastatic progression. Cancer Cell. 2005; 8:393–406. doi:10.1016/j.ccr.2005.10.001. [PubMed: 16286247]
21. Wallace TA, et al. Tumor immunobiological differences in prostate cancer between African-American and European-American men. Cancer Res. 2008; 68:927–936. doi:10.1158/0008-5472.CAN-07-2608. [PubMed: 18245496]
22. Yu YP, et al. Gene expression alterations in prostate cancer predicting tumor aggression and preceding development of malignancy. J Clin Oncol. 2004; 22:2790–2799. doi:10.1200/JCO.2004.05.158. [PubMed: 15254046]
23. Lin CY, et al. Discovery of estrogen receptor alpha target genes and response elements in breast tumor cells. Genome biology. 2004; 5:R66. doi:10.1186/gb-2004-5-9-r66. [PubMed: 15345050]
24. Romano A, et al. Identification of novel ER-alpha target genes in breast cancer cells: gene- and cell-selective co-regulator recruitment at target promoters determines the response to 17beta-estradiol and tamoxifen. Molecular and cellular endocrinology. 2010; 314:90–100. doi:10.1016/j.mce.2009.08.008. [PubMed: 19698761]
25. Yu J, et al. An integrated network of androgen receptor, polycomb, and TMPRSS2-ERG gene fusions in prostate cancer progression. Cancer cell. 2010; 17:443–454. doi:10.1016/j.ccr.2010.03.018. [PubMed: 20478527]
26. Giannopoulou EG, Elemento O. An integrated ChIP-seq analysis platform with customizable workflows. BMC bioinformatics. 2011; 12:277. doi:10.1186/1471-2105-12-277. [PubMed: 21736739]
27. Bond CS, Fox AH. Paraspeckles: nuclear bodies built on long noncoding RNA. J Cell Biol. 2009; 186:637–644. doi:10.1083/jcb.200906113. [PubMed: 19720872]
28. Holzbeierlein J, et al. Gene expression analysis of human prostate carcinoma during hormonal therapy identifies androgen-responsive genes and mechanisms of therapy resistance. Am J Pathol. 2004; 164:217–227. doi:10.1016/S0002-9440(10)63112-4. [PubMed: 14695335]
29. Magee JA, et al. Expression profiling reveals hepsin overexpression in prostate cancer. Cancer Res. 2001; 61:5692–5696. [PubMed: 11479199]
30. Tamura K, et al. Molecular features of hormone-refractory prostate cancer cells by genome-wide gene expression profiles. Cancer Res. 2007; 67:5117–5125. doi:10.1158/0008-5472.CAN-06-4040. [PubMed: 17545589]
31. Welsh JB, et al. Analysis of gene expression identifies candidate markers and pharmacological targets in prostate cancer. Cancer Res. 2001; 61:5974–5978. [PubMed: 11507037]
32. Barbieri CE, et al. Exome sequencing identifies recurrent SPOP, FOXA1 and MED12 mutations in prostate cancer. Nature genetics. 2012; 44:685–689. doi:10.1038/ng.2279. [PubMed: 22610119]
33. Cerami E, et al. The cBio cancer genomics portal: an open platform for exploring multidimensional cancer genomics data. Cancer Discov. 2012; 2:401–404. doi:10.1158/2159-8290.CD-12-0095. [PubMed: 22588877]
34. Gao J, et al. Integrative analysis of complex cancer genomics and clinical profiles using the cBioPortal. Sci Signal. 2013; 6:pl1. doi:10.1126/scisignal.2004088. [PubMed: 23550210]
35. Erho N, et al. Discovery and Validation of a Prostate Cancer Genomic Classifier that Predicts Early Metastasis Following Radical Prostatectomy. PLoS One. 2013; 8:e66855. doi:10.1371/journal.pone.0066855. [PubMed: 23826159]
36. Karnes RJ, et al. Validation of a Genomic Classifier that Predicts Metastasis Following Radical Prostatectomy in an At Risk Patient Population. J Urol. 2013 doi:10.1016/j.juro.2013.06.017.
37. Rickman DS, et al. ERG cooperates with androgen receptor in regulating trefoil factor 3 in prostate cancer disease progression. Neoplasia. 2010; 12:1031–1040. [PubMed: 21170267]
38. Nakagawa S, Naganuma T, Shioi G, Hirose T. Paraspeckles are subpopulation-specific nuclear bodies that are not essential in mice. J Cell Biol. 2011; 193:31–39. doi:10.1083/jcb.201011110. [PubMed: 21444682]
39. Guttman M, et al. Chromatin signature reveals over a thousand highly conserved large non-coding RNAs in mammals. Nature. 2009; 458:223–227. doi:10.1038/nature07672. [PubMed: 19182780]

40. Burger MJ, et al. Expression analysis of delta-catenin and prostate-specific membrane antigen: their potential as diagnostic markers for prostate cancer. Int J Cancer. 2002; 100:228–237. doi: 10.1002/ijc.10468. [PubMed: 12115574]
41. Gumulec J, et al. Evaluation of alpha-methylacyl-CoA racemase, metallothionein and prostate specific antigen as prostate cancer prognostic markers. Neoplasma. 2012; 59:191–201. [PubMed: 22248277]
42. Jiang N, Zhu S, Chen J, Niu Y, Zhou L. A-Methylacyl-CoA Racemase (AMACR) and Prostate-Cancer Risk: A Meta-Analysis of 4,385 Participants. PLoS One. 2013; 8:e74386. doi:10.1371/journal.pone.0074386. [PubMed: 24130666]
43. Ross JS, et al. Correlation of primary tumor prostate-specific membrane antigen expression with disease recurrence in prostate cancer. Clin Cancer Res. 2003; 9:6357–6362. [PubMed: 14695135]
44. Xiao Z, et al. Quantitation of serum prostate-specific membrane antigen by a novel protein biochip immunoassay discriminates benign from malignant prostate disease. Cancer Res. 2001; 61:6029–6033. [PubMed: 11507047]
45. Chu C, Quinn J, Chang HY. Chromatin isolation by RNA purification (ChIRP). Journal of visualized experiments : JoVE. 2012 doi:10.3791/3912.
46. Bernstein E, Allis CD. RNA meets chromatin. Genes Dev. 2005; 19:1635–1655. doi:10.1101/gad.1324305. [PubMed: 16024654]
47. Khalil AM, et al. Many human large intergenic noncoding RNAs associate with chromatin-modifying complexes and affect gene expression. Proc Natl Acad Sci U S A. 2009; 106:11667–11672. doi:10.1073/pnas.0904715106. [PubMed: 19571010]
48. Tsai MC, et al. Long noncoding RNA as modular scaffold of histone modification complexes. Science. 2010; 329:689–693. doi:10.1126/science.1192002. [PubMed: 20616235]
49. Wang KC, et al. A long noncoding RNA maintains active chromatin to coordinate homeotic gene expression. Nature. 2011; 472:120–124. doi:10.1038/nature09819. [PubMed: 21423168]
50. Bonkhoff H, Fixemer T, Hunsicker I, Remberger K. Estrogen receptor expression in prostate cancer and premalignant prostatic lesions. Am J Pathol. 1999; 155:641–647. doi:S0002-9440(10)65160-7 [pii] 10.1016/S0002-9440(10)65160-7. [PubMed: 10433957]
51. Setlur SR, et al. Estrogen-dependent signaling in a molecularly distinct subclass of aggressive prostate cancer. J Natl Cancer Inst. 2008; 100:815–825. doi:djn150 [pii] 10.1093/jnci/djn150. [PubMed: 18505969]
52. Singh PB, Matanhelia SS, Martin FL. A potential paradox in prostate adenocarcinoma progression: oestrogen as the initiating driver. Eur J Cancer. 2008; 44:928–936. doi:10.1016/j.ejca.2008.02.051. [PubMed: 18381236]
53. Nicolaiew N, et al. Association between estrogen and androgen receptor genes and prostate cancer risk. Eur J Endocrinol. 2009; 160:101–106. doi:10.1530/EJE-08-0321. [PubMed: 18952763]
54. Gibb EA, et al. Human cancer long non-coding RNA transcriptomes. PLoS One. 2011; 6:e25915. doi:10.1371/journal.pone.0025915. [PubMed: 21991387]
55. Amaral PP, Clark MB, Gascoigne DK, Dinger ME, Mattick JS. lncRNAdb: a reference database for long noncoding RNAs. Nucleic Acids Res. 2011; 39:D146–151. doi:10.1093/nar/gkq1138. [PubMed: 21112873]
56. Benjamini Y, Hochberg Yosef. Controlling the False Discovery Rate: A Practical and Powerful Approach to Multiple Testing. Journal of the Royal Statistical Society. Series B (Methodological). 1995; 57:289–300.
57. Rhodes DR, et al. ONCOMINE: a cancer microarray database and integrated data-mining platform. Neoplasia. 2004; 6:1–6. [PubMed: 15068665]
58. Blute ML, Bergstralh EJ, Iocca A, Scherer B, Zincke H. Use of Gleason score, prostate specific antigen, seminal vesicle and margin status to predict biochemical failure after radical prostatectomy. J Urol. 2001; 165:119–125. doi:10.1097/00005392-200101000-00030. [PubMed: 11125379]

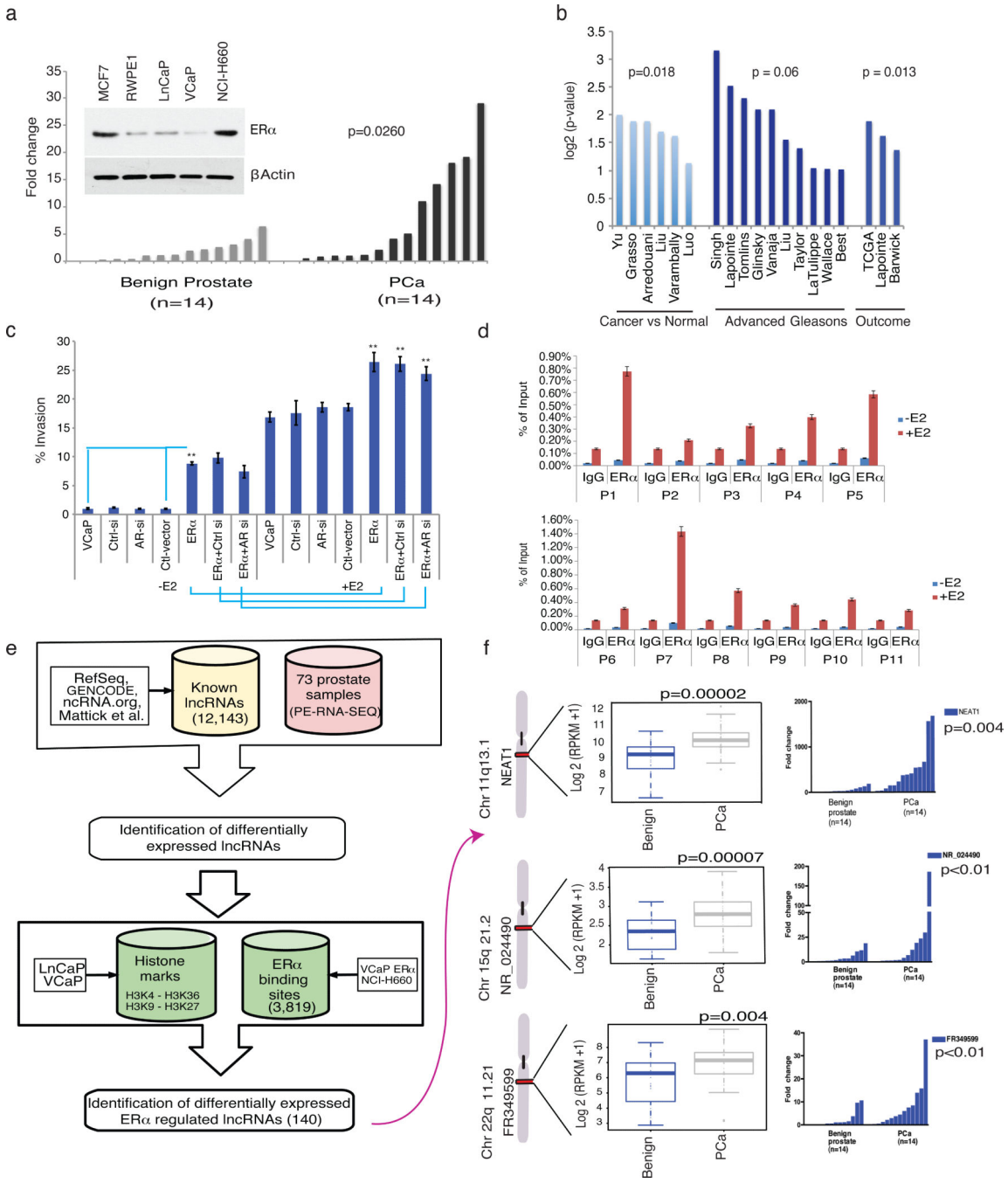

Figure 1. ERα plays a distinct role in prostate cancer

(a) ERα is upregulated in prostate cancer compared with matched benign controls. Waterfall plots depict the qPCR expression levels of ERα mRNA in an independent cohort of benign (n=14) and PCa (n=14). (inset A) The expression of ERα in different prostate cancer cell lines was determined by western blotting and compared with MCF7, a breast cancer cell line. (b) Analysis of ERα expression in Oncomine public datasets of normal vs. prostate cancer and advanced disease (c) Invasion of VCaP and VCaP ERα cells analyzed 48 hrs post-treatment with vehicle control or E2 (10nM) in presence of control or AR-siRNA.

Results are expressed as the mean±s.d. of three independent experiments. Student's *t*-test was performed for comparisons (% Invasion) between –E2 and +E2 conditions for ERα, ERα-Ctrl siRNA and AR-siRNA and *p<0.05 and **p<0.01 was considered statistically significant. Error bars represent the range of data. (d) Recruitment of endogenous ERα to target gene chromatin was analyzed in VCaP cells with or without E2 treatment. Results are expressed as the means of percentage of input ±s.d. of two independent experiments. Error bars represent the range of data. (e) Computational pipeline for identification of $ER\tilde{\alpha}\mathrm{regulated}$ lncRNAs upregulated in prostate cancer: A schematic overview of the methodology employed to identify ERα-regulated lncRNAs that are differentially expressed between benign vs. prostate cancer and prostate cancer vs. NEPC. (f) Box plots show expression levels of the top three $ER\tilde{\alpha}\mathrm{regulated}$ lncRNAs from 26 benign and 40 PCa cases, with ideogram depicting their chromosomal position. Waterfall plots depict the qPCR expression levels on an independent cohort of benign (n=14) and PCa (n=14) of the three nominated lncRNAs: NEAT1, NR_024490, and FR349599.

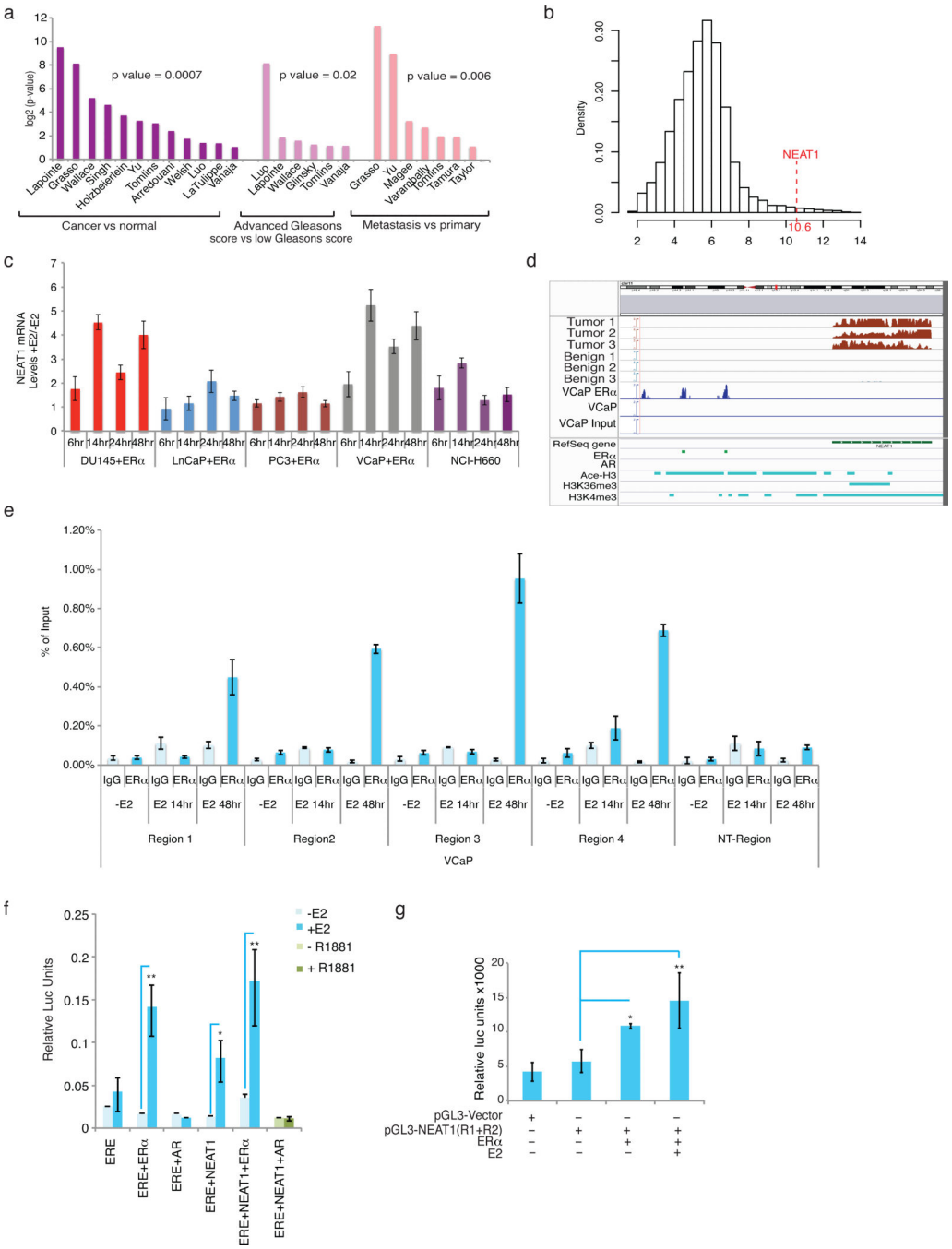

Figure 2. ERα regulated NEAT1 lncRNA is upregulated in prostate cancer

NEAT1 is overexpressed in various prostate datasets (Oncomine). (b) Distribution of the median expression of all genes (core transcript clusters) on the Human Exon 1.0 ST array in the pooled Mayo Clinic cohort (n = 594). NEAT1's expression ranks in the 99th percentile of all genes on the array. (c) Expression of NEAT1 with/without ERα overexpression and E2 treatment (10nM) at different time points in a panel of prostate cancer cell lines. Results are expressed as the mean±s.d. of three independent experiments (d) View of NEAT1 genomic location indicates presence of two ERα binding sites in the promoter region. Read

coverage tracks derived from RNA sequencing data indicates higher abundance of NEAT1 transcripts in PCa compared to benign tumors in 3 representative cases. The figure also reports the ChIP sequencing coverage tracks for ERα (VCaP ERα, VCaP and input DNA as control). The bottom panel shows the binding sites of ERα, AR (from Yu et al, GEO Accession GSM353651 - tissue AR), Ace-H3, H3K4me3 and H3K36me3 in VCaP cell line (from Yu et al, GEO Accession GSM353629, GSM353620 and GSM353624), respectively. (e) Chromatin immunoprecipitation followed by quantitative PCR to study ERα recruitment to NEAT1 promoter in VCaP cells with/without E2 treatment (10nM) was performed with primers spanning the binding regions identified by ERα ChIP-seq data. Primers for non-specific region were used as negative control for ChIP studies. Results are expressed as the means of percentage of input ±s.d. of two independent experiments. Vertical error bars represent the range of data. (f) Luciferase based promoter reporter assays was utilized to analyze effect of ERα and/or AR on ERE-Luc promoter in VCaP cells. Cells were transiently transfected with the (ERE)3-SV40-luc reporter plasmid and/or ERα and/or AR treated with/without E2 or R1881 (1nM) for 48 h. Results are expressed as the mean±s.d calculated from three independent experiments. (g) Luciferase based promoter reporter assays was utilized to analyze NEAT1 promoter activity following ERα expression -/+E2 (10 nM) for 24 hr. Results are expressed as the means±s.d. calculated from three independent experiments. Error bars represent the range of data. Student's *t*-test was performed for comparisons where indicated and *p<0.05 and **p<0.01 was considered statistically significant.

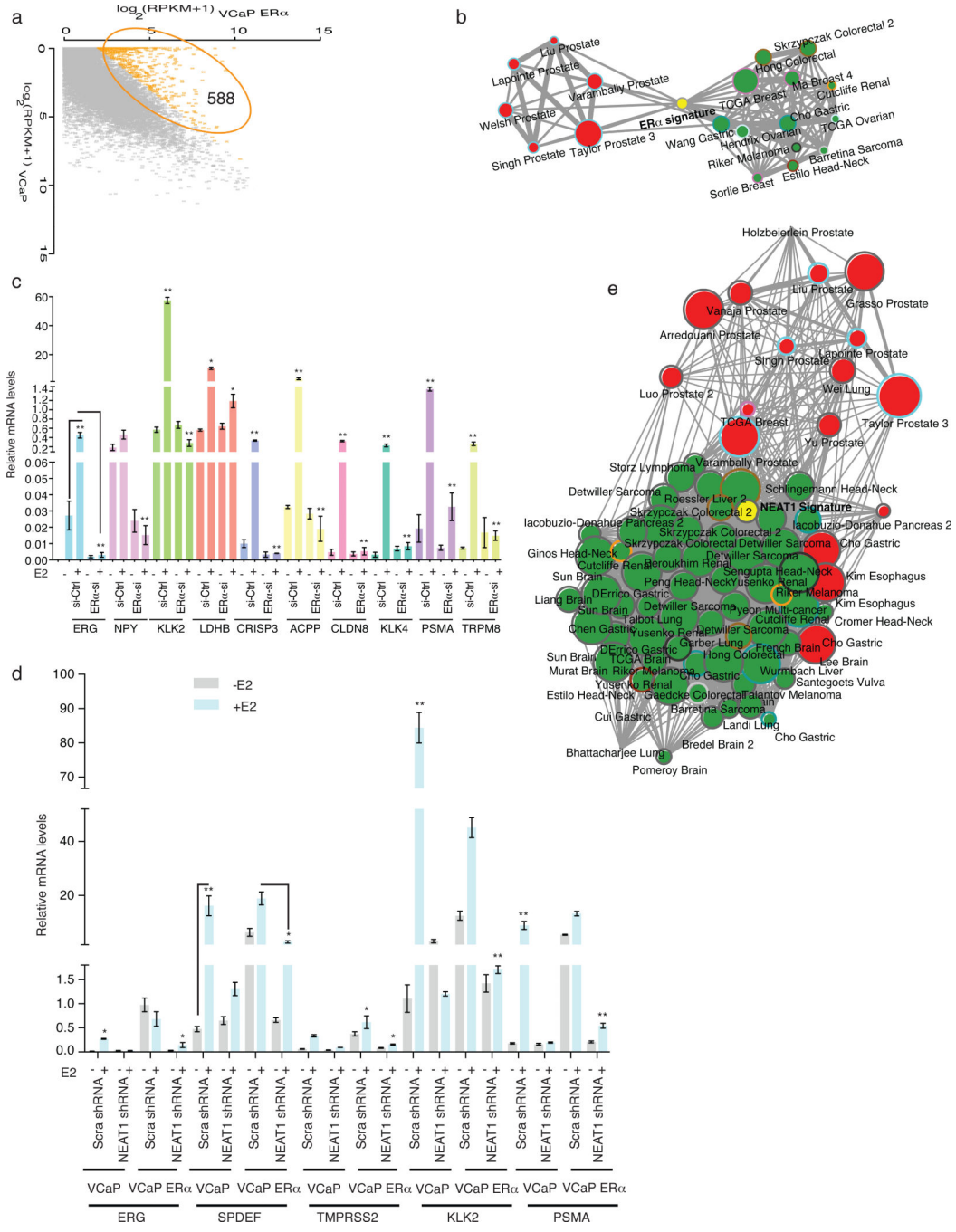

Figure 3. NEAT1 ERα signature correlates with prostate cancer

(a) Scatter plots for gene expression levels in VCaP ERα compared to VCaP cell lines. (b) 588 genes that are overexpressed in VCaP ERα (log2 fold change > 2) were used for Oncomine concept analysis across different cancer datasets (see Methods for detail). (c) qRT-PCR analysis of relative mRNA levels of ERα target genes in VCaP cells with knockout of ERα with and without E2 treatment. The target genes selected for validation are the ones that had the highest log2 fold difference in VCaP and VCaP ERα cell lines. Results are expressed as the mean±s.d. calculated from three independent experiments. Student's *t*-

test was performed (as indicated) for comparisons between - E2 and +E2 conditions for Ctrl siRNA and ERα-siRNA transfections and *p<0.05 and **p<0.01 was considered statistically significant. A representative example is shown for ERG target expression. Vertical error bars represent the range of data. (d) qRT-PCR analysis of ERα target genes in VCaP cells with ERα overexpression and NEAT1 knockout with and without E2 treatment. Results are expressed as the mean±s.d. calculated from three independent experiments. Error bars represent the range of data. Student's *t*-test was performed for comparisons between – E2 and +E2 conditions for scrambled shRNA and NEAT1 shRNA transfections in VCaP and VCaP ERα cells and *p<0.05 and **p<0.01 was considered statistically significant. Vertical error bars represent the range of data. A representative example is shown for SPDEF target expression. (e) Network representation of NEAT1 signature, derived from genes overexpressed in VCaP NEAT1 (NEAT1 signature) cells, across different cancer datasets using Oncomine concept analysis.

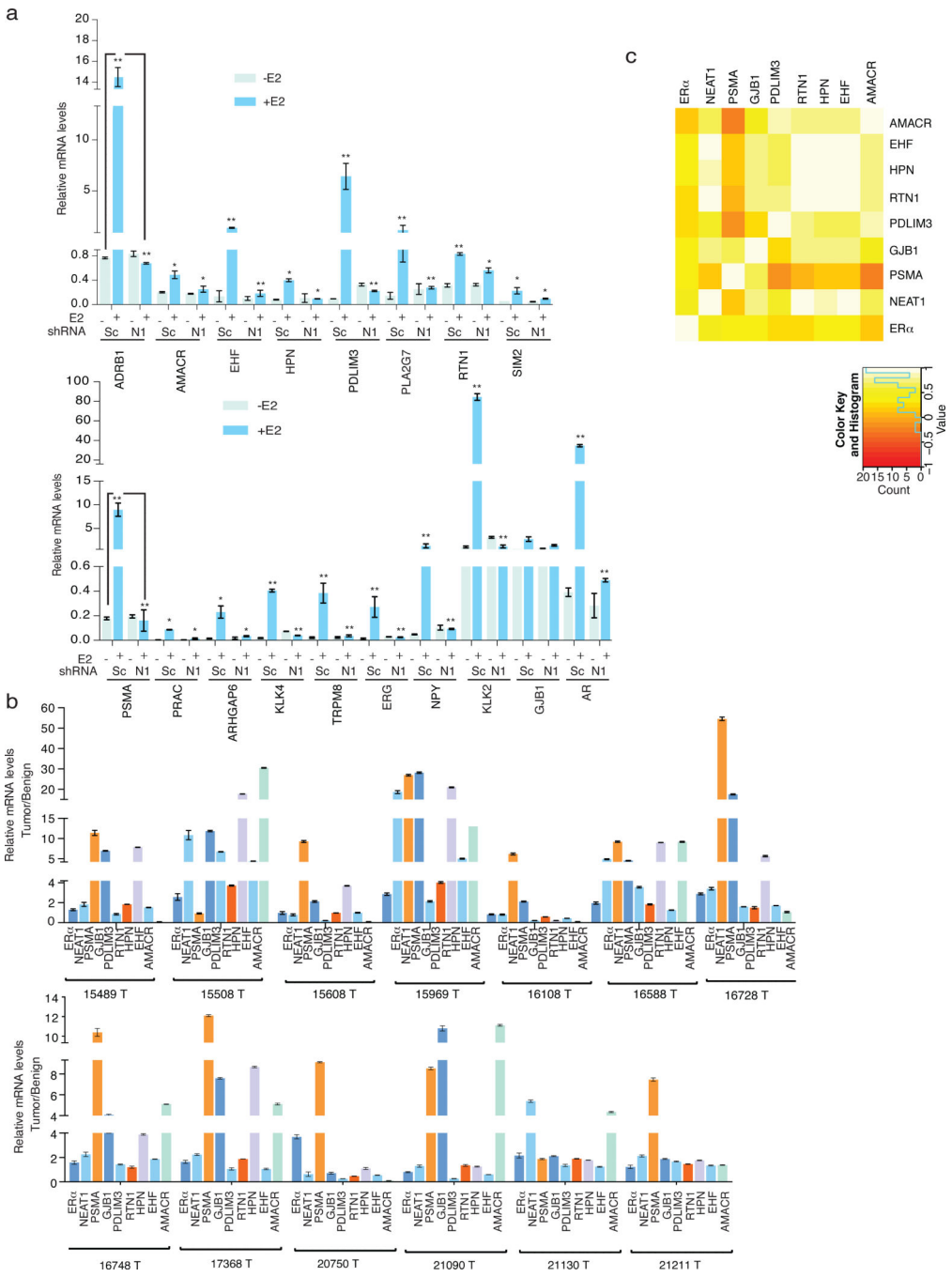

Figure 4. NEAT1 ERα signature is upregulated in prostate cancer

(a) Relative mRNA levels of genes nominated from analysis in Fig. 3b and 3e, analyzed using qRT-PCR in parental VCaP cells transfected with scrambled (Sc) and NEAT1 shRNA (N1) respectively with and without E2 (10nM) treatment. Results are expressed as the mean ±s.d. calculated from three independent experiments. Error bars represent the range of data. Student's *t*-test was performed for comparisons (relative mRNA levels of target gene expression) between –E2 and +E2 conditions for scrambled shRNA and NEAT1 shRNA transfections. A representative example is shown for ADRB1 and PSMA target expression.

*p<0.05 and **p<0.01 was considered statistically significant. (b) Validation of expression of the top target NEAT1 ERα signature genes in a small matched patient cohort of 13 benign and 13 PCa, n=26. Results are expressed as the mean±s.d. of two independent experiments. Error bars represent the range of data. (c) Heatmap shows the Spearman's correlation results from (b).

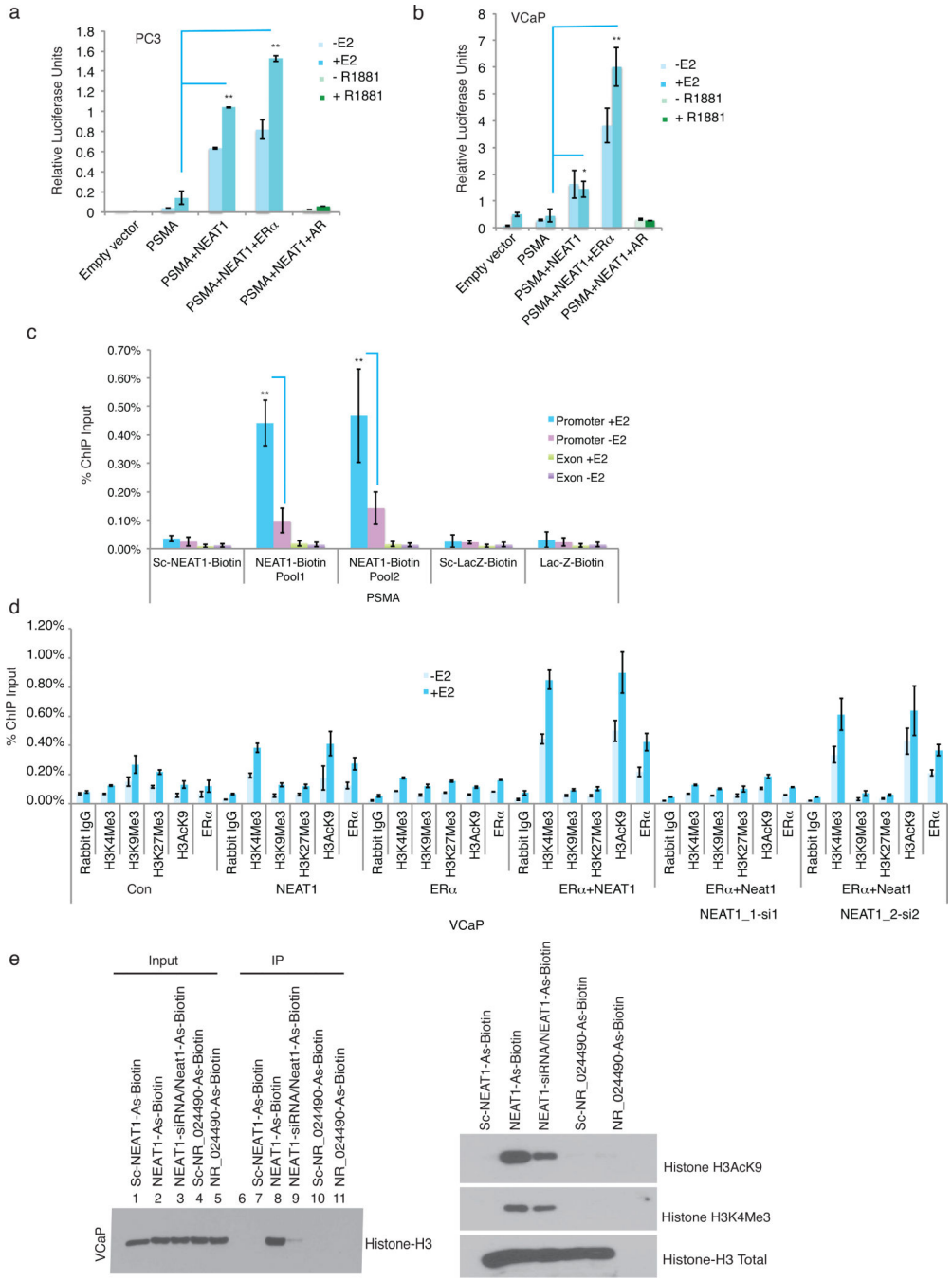

Figure 5. NEAT1 is a transcriptional regulator

(a & b) Promoter luciferase reporter assay shows that NEAT1 activates PSMA promoter in PC3 and VCaP cells. Cells were co transfected with empty vector or PSMA luc and Renilla-luc reporter genes alone or with NEAT1, NEAT1+ERα and NEAT1+AR. Luciferase activity was measured 48h post treatment with E2 (10nM) or R1881 (1nM). Results are expressed as the mean±s.d. calculated from three independent experiments. Student's *t*-test was performed for comparisons (relative PSMA-luciferase activity) between –E2 and +E2 conditions for vector control, NEAT1 and NEAT1+ERα transfections in PC3 and VCaP

cells. *p<0.05 and **p<0.01 was considered statistically significant. (c) Quantitative analysis of NEAT1 ChIRP in VCaP cells with or without E2 treatment (10nM). Recruitment profiles of NEAT1 to PSMA are shown. Results are expressed as the means of percentage of input ±s.d calculated from two independent experiments. Error bars represent the range of data. Results were reproducible between representative experiments. **p<0.01 was considered statistically significant. (d) Analysis of chromatin landscape at PSMA promoter performed by ChIP in VCaP cells alone or transected with NEAT1, ERα, NEAT1 ERα, NEAT1 ERα NEAT1_1 siRNA, NEAT1 ERα NEAT1_2 siRNA with and without E2 treatment. qPCR was performed with specific primers for the PSMA promoter. Results are expressed as the means of percentage of input ±s.d. calculated from two independent experiments. Error bars represent the range of data. Results were reproducible between representative experiments. (e) NEAT1 binds to Histone H3. 20 mer biotinylated NEAT1 and NR_024490 antisense probes were used to immunoprecipitate NEAT1 and NR_024490 from nuclear lysates of VCaP cells using streptavidin-magnetic beads. Immunoprecipitates from Streptavidin-IP were analyzed on 15% gel and probed for Histone H3. NEAT1 is shown to also bind with active histone H3 modifications including, H3AcK9 and H3K4Me3.

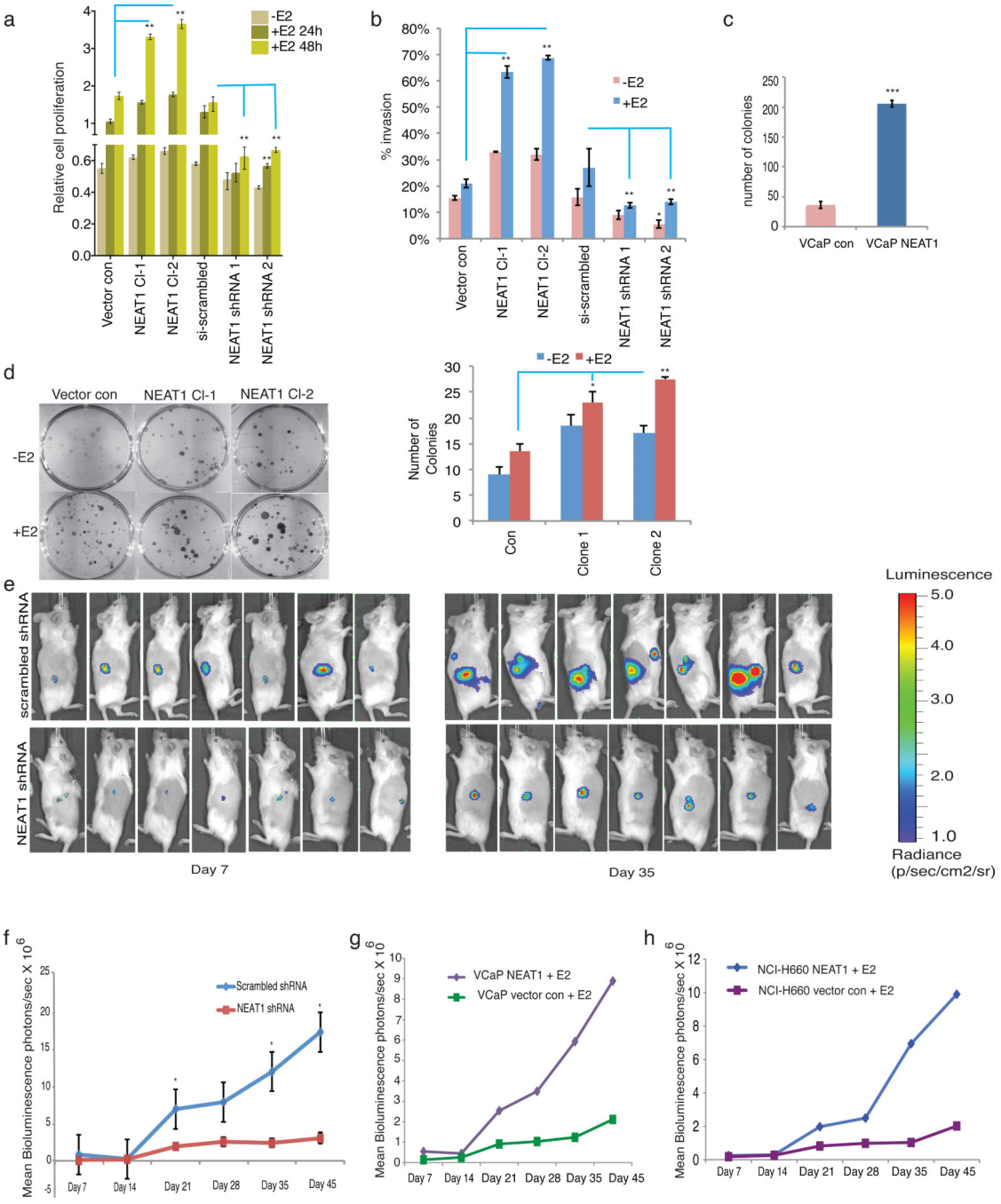

Figure 6. NEAT1 is a driver of oncogenic cascade

(a) Cell proliferation assays were performed in VCaP vector control, NEAT1 overexpressing cells and also in si scrambled and NEAT1 knockout cells with or without E2 treatment (10nM) at 24h and 48h time points. Results are expressed as the mean±s.d. calculated from three independent experiments. Student's *t*-test was performed for comparisons (relative cell proliferation) between E2 conditions for vector control, NEAT1 Cl-1 and NEAT1 Cl-2 and E2 conditions for si-scrambled, Neat1-shRNA1 and shRNA2 transfections. **p<0.01 was considered statistically significant (b) Quantitative bar chart for depicting percentage cell

invaded at the completion of invasion assay performed in VCaP vector control, NEAT1 overexpressing cells and also in si scrambled and NEAT1 knockout cells with or without E2 treatment (10nM). Results are expressed as the mean±s.d. of three independent experiments. *p<0.05 and **p<0.01, Student's *t*-test. (c) Soft agar assays were performed with VCaP control and NEAT1 expressing cells. Quantitative bar-plot analysis of stained colonies at 21 days are shown. Results are expressed as the mean±s.d. of three independent experiments. ***p<0.001, Student's *t*-test. (d) Colony forming assay were performed in VCaP vector control, NEAT1 overexpressing cells with or without E2 treatment (10nM). Right panel depicts the number of colonies at 21 days. Results are expressed as the mean±s.d. calculated from three independent experiments. *p<0.05 and **p<0.01, Student's *t*-test. (e) VCaP ERα cells expressing con shRNA luciferase (luc) and NEAT1 shRNA luc were injected s/c into the flank of male NOD-SCID mouse. Bioluminescent imaging on Day 7 and Day 35 in the VCaP ERα scrambled shRNA (top panel) and VCaP ERα NEAT1 shRNA (bottom panel) injected mice is shown. (f) Growth curve for the tumors monitored upto 45 days. Results are expressed as the mean±s.d. calculated from three independent experiments. *p<0.05, Student's *t*-test. (g & h) VCaP and NCI-H660 vector control and NEAT1 overexpressing cells were injected s/c into the flank of male NODSCID mouse. Bioluminescence imaging monitored the tumor growth. Growth curve for the tumors monitored upto 45 days is shown, VCaP (g) and NCI-H660 (h).

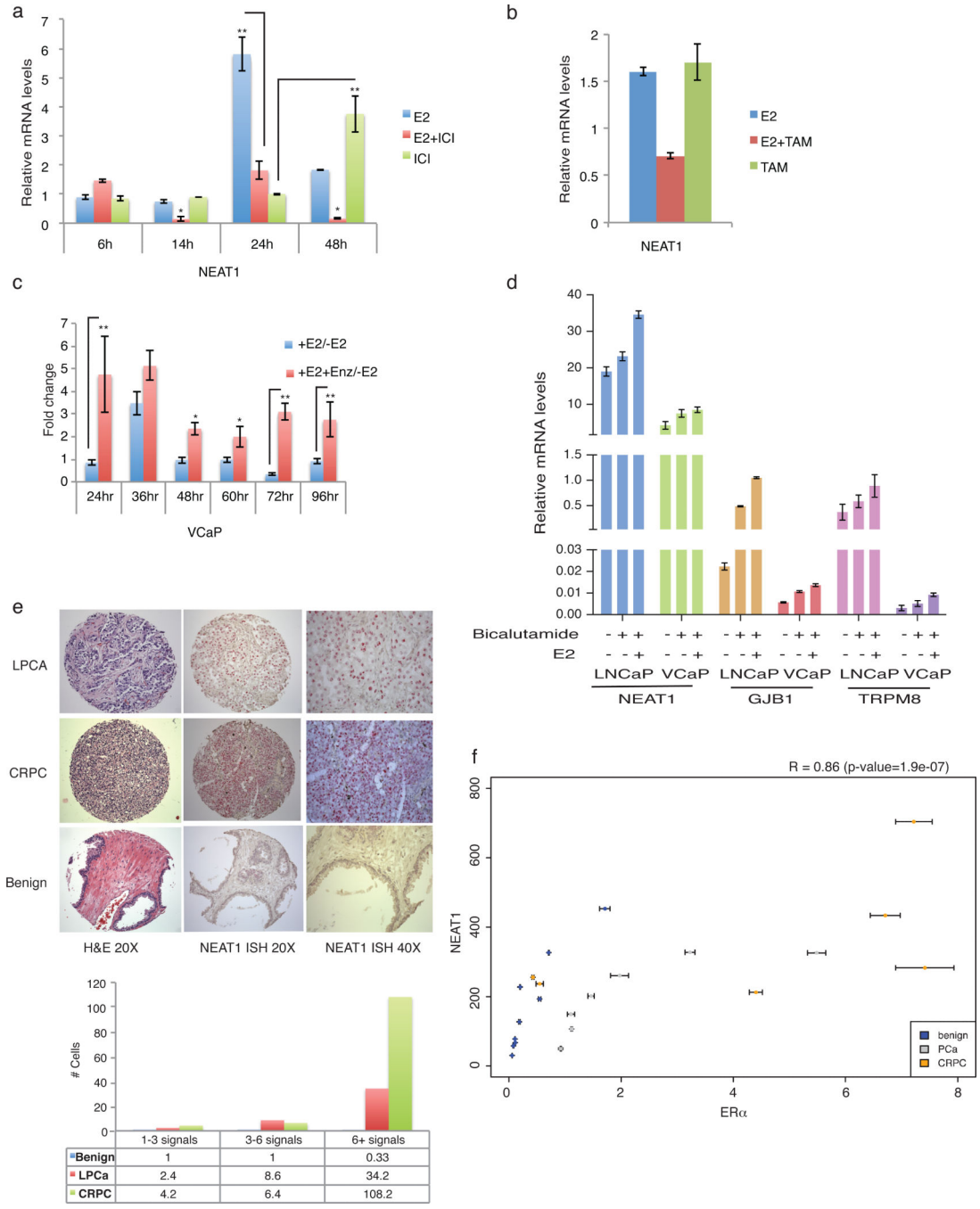

Figure 7. NEAT1 in therapy resistance

(a) NEAT1 expression in VCaP cells treated with E2 (10nM) at different time points alone, E2 + ICI (10nM + 10μM) or ICI (10μM) alone. Results are expressed as the mean±s.d. of three independent experiments. * $p < 0.05$, ** $p < 0.01$, Student's t-test (b) NEAT1 expression in VCaP cells treated with E2, E2 + 4OHT (10nM + 10nM), and 4OHT (10nM) alone for 48h. (c) NEAT1 expression in VCaP cells treated with or without E2 (10nM) or E2 + Enzalutamide (10nM + 10μM) at different time points. Results are expressed as the mean ±s.d. of three independent experiments. *p<0.05 and **p<0.01, Student's *t*-test. (d) qRT-

PCR analysis of NEAT1, GJB1 and TRPM8 in LnCaP and VCaP control cells, with bicalutamide treatment (10μM) alone or in combination with E2 (10nM) for 48h. Results are expressed as the means±s.d. of three independent experiments. Vertical bars represent range of data. Results were reproducible between representative experiments. (e) Representative image for RNA ISH of NEAT1 in benign, localized PCa and in advanced disease (top panel). Quantitation for the RNA ISH signals shown in the bottom using RNA Spot Studio (f) Scatter plot showing the correlation between ERα and NEAT1 expression by qRT PCR in 9 cases of benign prostate, 7 PCa, and 7 CRPC. Pearson's correlation coefficient R = 0.86 (p-value=1.9e-07).

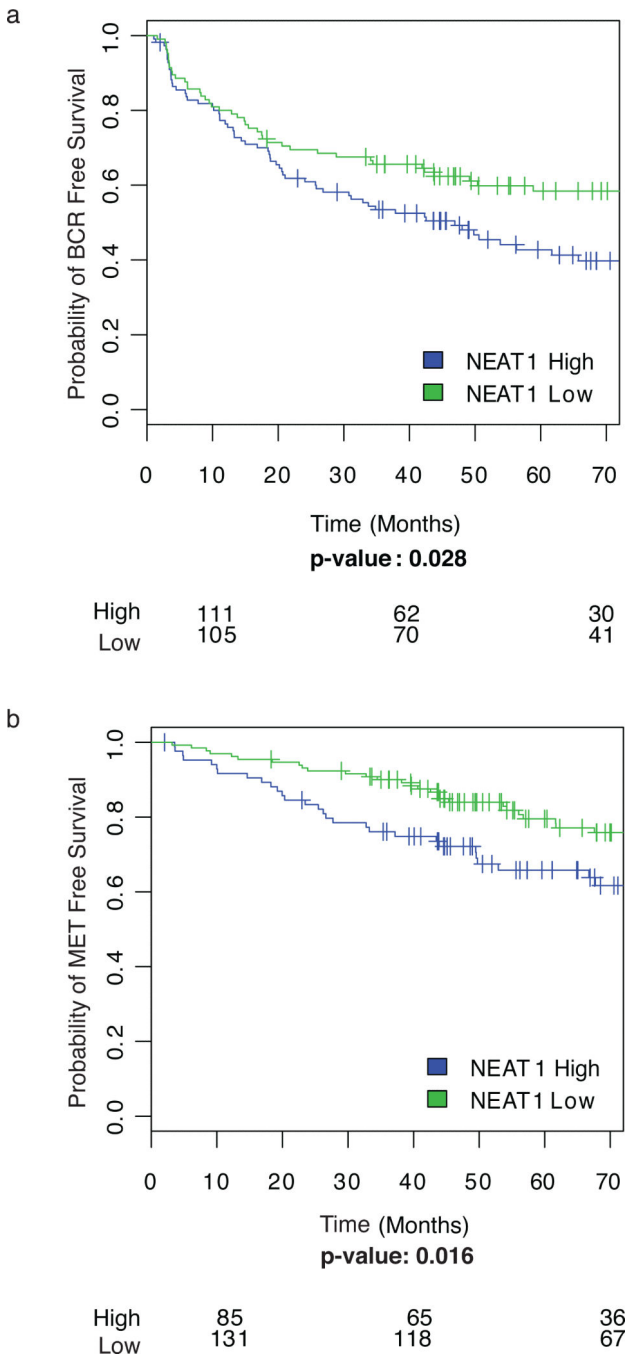

Figure 8. NEAT1 overexpression is associated with aggressive prostate cancer

(a-b) Kaplan Meier curves showing (a) Biochemical recurrence (BCR) free survival and (b) metastatic recurrence (MET) free survival for NEAT1 low and high expression groups of samples from the Mayo case-cohort dataset [35](n = 216). The cut points to define high and low NEAT1 expression were selected using patients from the Mayo nested case-control dataset (n = 378) [58] by maximizing the product of the sensitivity and specificity for each endpoint. The number of patients at risk for each group is shown beneath the plot.

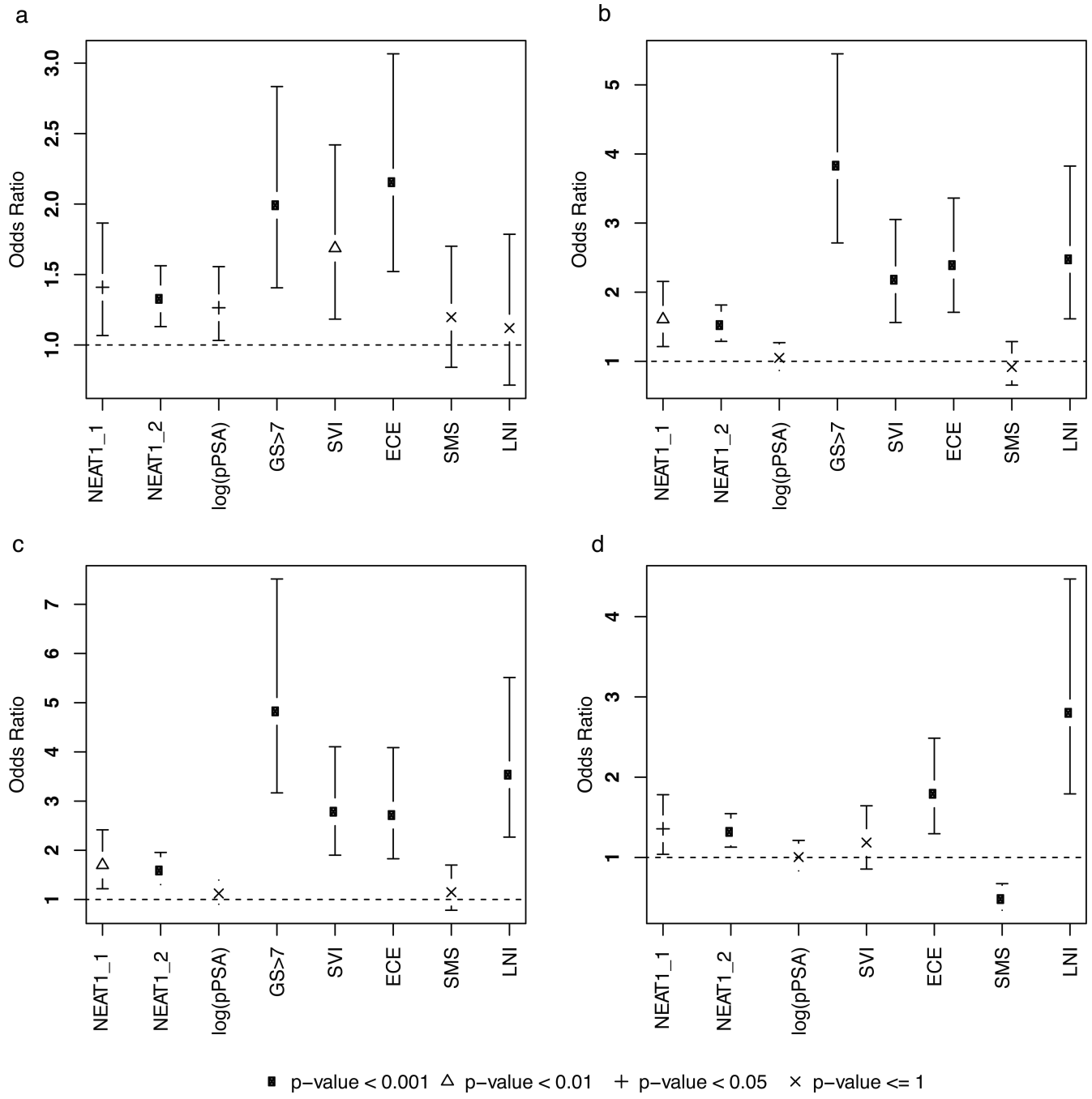

Figure 9. NEAT1 is a strong prognosticator of prostate cancer

(a-d) Univariable forest plots comparing the expression of NEAT1's short (NEAT1_1) and long isoform (NEAT1_2) to clinicopathologic variables in the pooled Mayo cohort (n = 594) (a) BCR, (b) MET, (c) prostate cancer specific mortality (PCSM), (d) Gleason score (GS) > 7. Pathological tumor stage 3 or greater (pT3+), Lymph Node Invasion (LNI), Surgical Margin Status (SMS) positive, Seminal Vesicle Invasion (SVI), Extra Capsular Extension (ECE), preoperative PSA (pPSA), adjuvant hormone therapy, and adjuvant radiation therapy are shown.

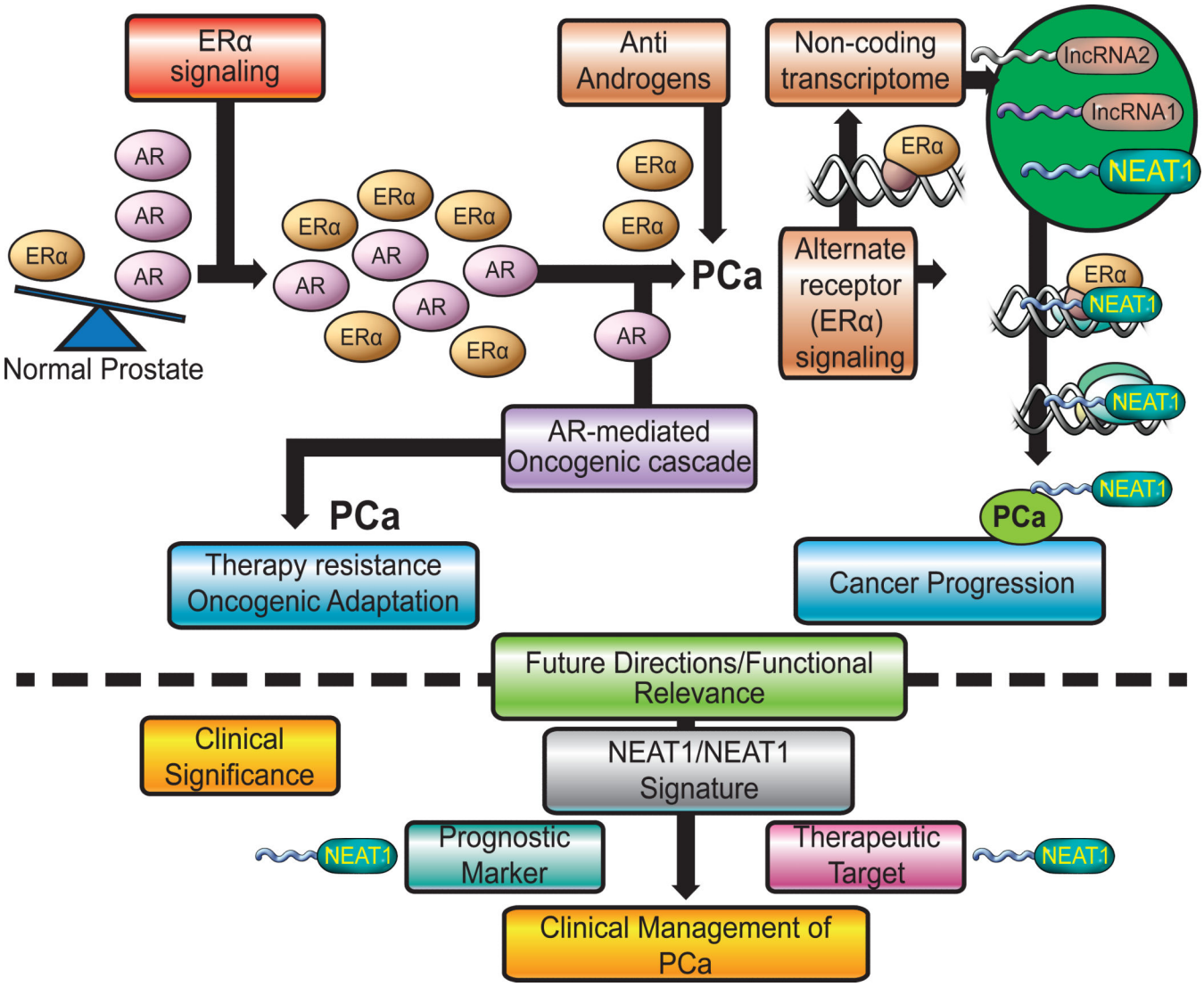

Figure 10. Model for NEAT1 function in prostate cancer

Functional ERα signaling in prostate cancer modulates expression of lncRNA NEAT1. Prostate epithelial cells positive for NEAT1 have oncogenic advantage and are refractile to androgen inhibitors or androgen ablation therapy. NEAT1 a histone interacting lncRNA and transcriptional regulator, is recruited to promoters of several prostate cancer specific genes. NEAT1 can modulate epigenetic landscape of target promoters and maintains expression of AR dependent and independent genes. Selection of alternate nuclear receptor signaling is a novel hallmark of prostate cancer progression.